



## Final Bachelor Thesis

---

# THERMAL ANALYSIS FOR THE TEIDESAT / ALISIO CUBESATS

---

### **Studies:**

Mechanical Engineering Bachelor

### **Author:**

Javier González Vilar

### **Tutors:**

Pablo Gustavo Redondo Caicoya

Pablo González de Chaves

Isabel Teresa Martín Mateos

**JUNE 2019**



*Page intentionally left in blank*

## Table of general contents

List of figures.....	4
List of tables.....	6
List of Abbreviations.....	7

## Report

0. Identification Page .....	3
1. Purpose.....	4
2. Scope .....	4
3. References .....	4
4. State of art .....	7
4.1. Teidesat.....	7
4.1.1. Introduction.....	7
4.1.2. Objectives of Teidesat.....	7
4.2. Satellite .....	7
4.3. CubeSat.....	9
4.4. Satellite subsystems .....	12
5. Solution analysis.....	16
5.1. Case plate.....	18
5.2. Sphere case .....	19
5.3. Cube case .....	20
5.4. All heat sources case.....	24
5.5. Case considering real surface.....	28
5.6. Cold case .....	21
5.7. ESATAN- TMS results .....	33
Teidesat case .....	34
ALISIO CASE .....	37

6. Conclusions and future work .....	40
--------------------------------------	----

## Annex 1: Calculations

1. Calculation from 4.5. developed .....	3
2. Times of eclipse .....	6

## Annex 2: ESATAN-TMS results

Teidesat case .....	1
ALISIO Case .....	11

## Annex 3: Theoretical context

1. Basics of Heat Transfer .....	3
2. Conduction .....	3
3. Convection .....	5
4. Radiation .....	6
4.1. The view factor .....	9
4.2. Heat transfer to or from a surface .....	11
4.3. Heat transfer between two surfaces .....	12
5. Orbits .....	13
6. Environments of Earth orbits .....	23
6.1. Direct solar .....	24
6.2. Albedo .....	26

6.3.	Earth IR.....	26
6.4.	Molecular free heating.....	27
6.5.	Charged-particle heating.....	28

## List of figures

### REPORT

Figure 1:	First artificial satellite, Sputnik [2] .....	8
Figure 2:	Equisat [5] .....	9
Figure 3:	CubeSat 1U [8] .....	11
Figure 4:	3U, 2U and 1U CubeSats [9].....	11
Figure 5:	Standard battery module for CubeSat [10].....	12
Figure 6:	1U CubeSat structure [11] .....	12
Figure 7:	Teidesat CubeSat scheme [8].....	12
Figure 8:	External structure of Teidesat satellite[11] .....	14
Figure 9:	Extreme position of the satellite illustrated by Eduardo Puyol Correa .....	26
Figure 10:	Surface properties by type of finish [19].....	28
Figure 11:	CubeSat face distribution.....	29
Figure 12:	Pharmasat [21] .....	31
Figure 13:	Temperature-time graph in one orbit .....	34
Figure 14:	Temperature-time graph in one orbit .....	35
Figure 15:	Teidesat temperature chart (-30°) .....	36
Figure 16:	Teidesat temperature chart (60°) .....	36
Figure 17:	Temperature-time graph in one orbit .....	37
Figure 18:	Temperature-time graph in one orbit .....	38
Figure 19:	Temperature-time graph in one orbit .....	39
Figure 20:	Temperature-time graph in one orbit .....	39
<b>ANNEX 1: Calculations</b>		
Figure 21:	Eclipse time vs Beta degree[12] .....	7

ANNEX 2: ESATAN-TMS

Figure 21: Material definition in ESATAN.....3

Figure 22: Optical set definition in ESATAN .....3

Figure 23: Cube definition in ESATAN .....4

Figure 24: Orbital parameters .....5

Figure 25: Orbital parameters .....6

Figure 26: Orbital parameters .....6

Figure 27: Pointing definition ESATAN.....7

Figure 28: Heat flux and orbital representation via ESATAN.....8

Figure 29: Input for the thermal analysis ESATAN.....9

Figure 30: Temperature-time graph in one orbit .....10

Figure 31: Temperature-time graph in one orbit .....11

Figure 32: Teidesat temperature chart (-30º) .....12

Figure 33: Teidesat temperature chart (60º) .....12

Figure 34: ALISIO geometry .....13

Figure 35: Temperature-time graph in one orbit .....14

Figure 36: Temperature-time graph in one orbit .....15

Figure 37: Temperature-time graph in one orbit .....16

Figure 38: Temperature-time graph in one orbit .....17

ANNEX 3: Theoretical context

Figure 39: Heat conduction through a large plane Wall [21] .....4

Figure 40: Thermal resistance [21] .....5

Figure 41: Blackbody radiation [21] .....6

Figure 42: The absorption of radiation incident on .....7

Figure 43: The effect of diffuse and gray approximations on the emissivity of a surface [21] .....8

Figure 44: Comparison of the emissivity of a real surface with those of a gray surface and a blackbody at the same temperature [21] .....8

Figure 45: The view factor [21].....9

Figure 46: Heat transfer between 2 surfaces [21] .....10

Figure 47: Surface resistance radiation [21].....11

Figure 48: Space resistance to radiation [21] ..... 12

Figure 49: Classical earth orbits [22]..... 13

Figure 50: Molniya orbit [22] ..... 14

Figure 51: Orbital Parameters [22] ..... 16

Figure 52: Total amount of time per orbit ..... 18

Figure 53: Orbit beta angle [22]..... 19

Figure 54: Eclipse durations [22] ..... 20

Figure 55: Cylinder in LEO [22] ..... 21

Figure 56: Seeing from the Sun beta changes [12] ..... 22

Figure 57: Heat sources [22]..... 23

Figure 58: Emittance vs Wavelength [22] ..... 24

Figure 59: Absorptance vs Wavelength [22] ..... 25

Figure 60: Eclipse time vs Beta degree[12] ..... 25

Figure 61: FMH ..... 28

List of tables

REPORT

Table 1: Temperatures of operation [12] ..... 12

Table 2: Conditions for each case ..... 15

Table 3: Results comparison ..... 19

Table 4: Temperature of a CubeSat with different coatings [17] ..... 20

Table 5: Parameters for the equation ..... 22

Table 6: Data for the equation ..... 23

Table 7: Temperature of a CubeSat for different material ..... 24

Table 8: Values for solar cells used in other space missions [17] ..... 26

Table 9: Temperatures for CubeSat with different combinations of surfaces ..... 28

Table 10: Data for the equation ..... 29

Table 11: Temperatures for CubeSat with different combinations of surfaces ..... 30



ANNEX 1: Calculations

Table 12: Anodize black combinations.....2

Table 13: Gold combinations.....3

Table 14: Alzac A-2 combinations.....3

Table 15: GSFC SiOx Al2O3-Ag combinations.....3

Table 16: Aclar film combinations .....4

Table 17: ATN black combinations.....4

ANNEX 3: Theoretical context

Table 18: LEO thermal Environment [23].....26

List of Abbreviations

ALISIO	Advanced Land Imaging Satellite for Infrared Observations
DRAGO	Demonstrator for Remote Analysis of Ground Observations
ECSS	European Cooperation for Space Standardization
ESA	European Space Agency
LEO	Low-Earth Orbit
NASA	National Aeronautics and Space Administration
TCS	Thermal Control System
NASA	National Aeronautics and Space Administration
AU	Astronomic unit
SWIR	Short Wave Infrared
1U	1 unit CubeSat
2U	2 unit CubeSat
3U	3 unit CubeSat
ISS	International Space Station





**Final Bachelor Thesis**

---

# THERMAL ANALYSIS FOR THE TEIDESAT / ALISIO CUBESATS

---

## **REPORT**

**Studies:**

Mechanical Engineering Bachelor

**Author:**

Javier González Vilar

**JUNE 2019**



*Page intentionally left in blank*

## Report

- 0. Identification Page.....3
- 1. Purpose.....4
- 2. Scope .....4
- 3. References .....5
- 4. State of art .....7
  - 4.1. Teidesat.....7
    - 4.1.1. Introduction.....7
    - 4.1.2. Objectives of Teidesat.....7
  - 4.2. Satellite .....7
  - 4.3. CubeSat.....9
  - 4.4. Satellite subsystems .....12
- 5. Solution analysis.....16
  - 5.1. Case plate.....18
  - 5.2. Sphere case .....19
  - 5.3. Cube case .....20
  - 5.4. All heat sources case.....24
  - 5.5. Case considering real surface.....28
  - 5.6. Cold case .....31
  - 5.7. ESATAN- TMS results .....33
  - Teidesat case .....34
  - ALISIO CASE .....37
- 6. Conclusions and future work .....40

## 0. Identification Page

Name of the project:	Thermal analysis for the Teidesat / Alisio CubeSat
Studies:	Mechanical engineering bachelor
Petitionary:	Instituto Astrofísico de Canarias
	Teidesat
Autor:	Javier González Vilar
Tutors:	Pablo Gustavo Redondo Caicoya
	Pablo González de Chaves
	Isabel Teresa Martín Mateos
Date:	14/06/2019



## 1. Purpose

The aim of this project is to analyse the temperature that a 1U CubeSat will encounter on orbit, and consequently produce a first approach to the thermal design of the satellite Teidesat.

The Microsatellite project team from IACTEC is also petitionary of this bachelor thesis because they are interested in performing thermal analysis in a CubeSat, so that they can develop their own nanosatellites. IACTec Microsatellites team is developing the Payload for a 3U CubeSat mission called ALISIO I, this case will be analysed too.

## 2. Scope

This project will be focused on the space segment, more concisely, the CubeSat thermal subsystem. A 1U CubeSat thermal analysis will be developed. However, the internal structure of the Teidesat CubeSat is not fully designed; so inner components will not be considered in this analysis.

After analysing different steady state models, transient stages will be analysed with the software ESATAN-TMS:

ITP Engines UK is kindly sponsoring Teidesat with the software licences for the analysis and simulation software ESATAN-TMS.



### 3. References

- [1] "Project Overview - TeideSat," 2019. [Online]. Available: <https://docs.google.com/document/d/1py2-e0ZOz14XUrZQTHbzpuHi6Hyft95ObaJLVr1Xfxg/edit#heading=h.raxjghua6tq0>. [Accessed: 13-Mar-2019].
- [2] "Fly Your Satellite! programme / CubeSats - Fly Your Satellite! / Education / ESA." [Online]. Available: [https://www.esa.int/Education/CubeSats\\_-\\_Fly\\_Your\\_Satellite/Fly\\_Your\\_Satellite!\\_programme](https://www.esa.int/Education/CubeSats_-_Fly_Your_Satellite/Fly_Your_Satellite!_programme). [Accessed: 29-Mar-2019].
- [3] S. May, "What Is a Satellite?," 2015.
- [4] G. Konecny, *Small satellites—A tool for Earth observation?* .
- [5] "About — CubeSat." [Online]. Available: <http://www.cubesat.org/about>. [Accessed: 13-Mar-2019].
- [6] A. Heiney, "ELaNa - Educational Launch of Nanosatellites," 2015.
- [7] "CubeSats - Fly Your Satellite! / Education / ESA." [Online]. Available: [https://www.esa.int/Education/CubeSats\\_-\\_Fly\\_Your\\_Satellite](https://www.esa.int/Education/CubeSats_-_Fly_Your_Satellite). [Accessed: 13-Mar-2019].
- [8] N. CubeSat Launch Initiative, "CubeSat 101: Basic Concepts and Processes for First-Time CubeSat Developers."
- [9] W. Lan, "CubeSat Design Specification Rev. 13 The CubeSat Program, Cal Poly SLO CubeSat Design Specification (CDS) REV 13 Document Classification X Public Domain ITAR Controlled Internal Only."
- [10] "Attitude Control and Determination System | Brown Space Engineering - Space For The People." [Online]. Available: <https://brownspace.org/acds/>. [Accessed: 13-Mar-2019].
- [11] L. Feria, P. Gustavo, and R. Caicoya, "Final Bachelor Thesis DESIGN OF THE MECHANICAL STRUCTURE FOR THE TEIDESAT Studies : Author : Tutors :," no. July, 2018.
- [12] G. Sebestyen, S. Fujikawa, N. Galassi, and A. Chuchra, *Low Earth Orbit Satellite Design*. 2018.



- [13] Wertz and Larson, *Space mission analysis and design workbook*. 2005.
- [14] “AZ Technology | Materials, Paint and Coatings: AZ-93 White Thermal Control, Electrically Conductive Paint / Coating (AZ’s Z-93P).” [Online]. Available: <http://www.aztechnology.com/materials-coatings-az-93.html>. [Accessed: 03-May-2019].
- [15] “Lord Aeroglaze® and Chemglaze® Coatings | Materials & Coatings for Aerospace, Defence, Energy & Electronics industries.” [Online]. Available: [https://www.pexa.com/products/space\\_optical\\_coatings/](https://www.pexa.com/products/space_optical_coatings/). [Accessed: 03-May-2019].
- [16] “Spacecraft External Temperatures.” [Online]. Available: [https://www.alternatewars.com/BBOW/Space/Spacecraft\\_Ext\\_Temps.htm](https://www.alternatewars.com/BBOW/Space/Spacecraft_Ext_Temps.htm). [Accessed: 13-Mar-2019].
- [17] J. H. Hemmer, “NASA Reference Publication 1121 Solar Absorptance and Thermal Emittance of Some Common Spacecraft Thermal-Control Coatings.”
- [18] E. Escobar, M. Diaz, and J. C. Zagal, “Evolutionary design of a satellite thermal control system: Real experiments for a CubeSat mission,” *Appl. Therm. Eng.*, vol. 105, pp. 490–500, 2016.
- [19] F. H. Perez, “Análisis Térmico De Un Satélite Del Tipo Cube Sat,” 2015.
- [20] S. Jos, “THERMAL MODELING OF NANOSAT A Thesis Presented to The Faculty of the Department of Mechanical and Aerospace Engineering,” no. May, 2012.
- [21] Y. A. Cengel, “Heat transfer, a practical approach.”
- [22] D. G. Gilmore, *Spacecraft Thermal Control Handbook Volume I : Fundamental Technologies*, vol. I. .
- [23] S. Scholarworks and D. Dinh, “Thermal Modeling of Nanosat,” 2012.



## 4. State of art

### 4.1. Teidesat

#### 4.1.1. Introduction

The project Teidesat was born as an initiative of students from the University of La Laguna who wanted to know more about Satellites and Space, which led to constitute a team whose objective is the design, construction, launch into orbit and operation of a nanosatellite based on the standard CubeSat. [1]

In order to fulfil this objective, the team is going to participate in the next “Fly your satellite!” call. In this program, the university student teams develop of their own satellite, whose mission is conceived at their own universities, and whose development is funded by the universities themselves and/or other national contributors [2].

Teidesat is the first project of the “Scientific-Technologic Association Hyperspace Canarias”.

#### 4.1.2. Objectives of Teidesat

The Teidesat team pursues the following objectives (not this project scope):

- Scientific objective: Establish optical communication of data download between the nanosatellite and Earth.
- Technologic objective: design and construct a nanosatellite that fulfils the quality standards of the European Space Agency (ESA).
- Academic objective: To learn about areas of knowledge related to space outside the academic discipline of each member, with the aim of becoming a much more complete and versatile professionals.
- Dissemination objective: the team believes in the importance of scientific-technical dissemination among people of all ages, but with special emphasis in the young. It devotes part of its time to this end trying to increase their interest in this topic.

### 4.2. Satellite

A satellite is a moon, planet or machine that orbits a planet or star. For example, Earth is a satellite because it orbits the Sun. Likewise, the moon is a satellite because it orbits Earth. Usually, the word "satellite" refers to a machine that is launched into space and moves around Earth or another body in space.





Earth and the moon are examples of natural satellites. Thousands of artificial, satellites orbit Earth, the first artificial satellite was the Sputnik I (figure 1) sent by the Soviet Union in 1957. Some take pictures of the planet that help meteorologists predict weather and track hurricanes. Some take pictures of other planets, the sun, black holes, dark matter or faraway galaxies. These pictures help scientists better understand the solar system and universe.

Other satellites are used mainly for communications, such as beaming TV signals and phone calls around the world. [3]



*Figure 1: First artificial satellite, Sputnik [2]*

Satellites are also classified according to its mass [4]:

- Large satellites: mass > 1000 kg
- Medium satellites: mass 500 to 1000 kg
- Mini satellites: mass 100 to 500 kg
- Micro satellites: mass 10 to 100 kg
- Nano satellites: mass 1 to 10 kg
- Pico satellites: mas 0.1 – 1 kg
- Femto satellites: mass < 100 g.



The standard CubeSat (which this project is based in) usually goes into the nanosatellite division.

Some advantages of using smaller spacecraft are:


- Constellations for low data rate communications
- Using formations to gather data from multiple points
- In-orbit inspection of larger satellites
- University-related research
- Testing or qualifying new hardware before using it on a more expensive spacecraft

#### 4.3. CubeSat

The CubeSat standard was created by California Polytechnic State University, San Luis Obispo and Stanford University's Space Systems Development Lab in 1999 to facilitate access to space for university students. Since then the standard has been adopted by hundreds of organizations worldwide. CubeSat developers include not only universities and educational institutions, like Brown university who developed Equisat (figure 2), but also private firms and government organizations [5].



Figure 2: Equisat [5]

Page: 10 of 40	Thermal analysis for the Teidesat / Alisio CubeSat	
----------------	--	---

The CubeSat standard facilitates frequent and affordable access to space with launch opportunities available on most launch vehicles [5].

Cubesats are a type of spacecraft that is affordable for students and small organizations, consequently different space agencies of the world have created space programs specifically for students, to develop this kind of spacecraft with their assistance.

For example, NASA students program is called ELaNa [6]. The ESA one is called Fly Your Satellite! [7].

Nevertheless, the cheap production of this kind of spacecraft makes also easier the access to space to other organizations, and so, it is being used all around the world in its different versions.

What makes this standard interesting is that, it must conform to specific criteria that control factors such as its shape, size, and weight. The very specific standards for CubeSats help reduce costs. The standardized aspects of CubeSats make it possible for companies to mass-produce them. As a result, the engineering and development of CubeSats becomes less costly than highly customized small satellites. The standardized shape and size also reduces costs associated with the development and the space launch.

CubeSats come in several sizes, which are based on the standard CubeSat “unit”—referred to as 1U. A 1U CubeSat is a 10x10x10 cm cube with a mass of approximately 1 to 1.33 kg (see figure 4). In the years since the CubeSat’s inception, larger sizes have become popular, such as the 1.5U, 2U, 3U, and 6U, but new configurations are always in development. [8]

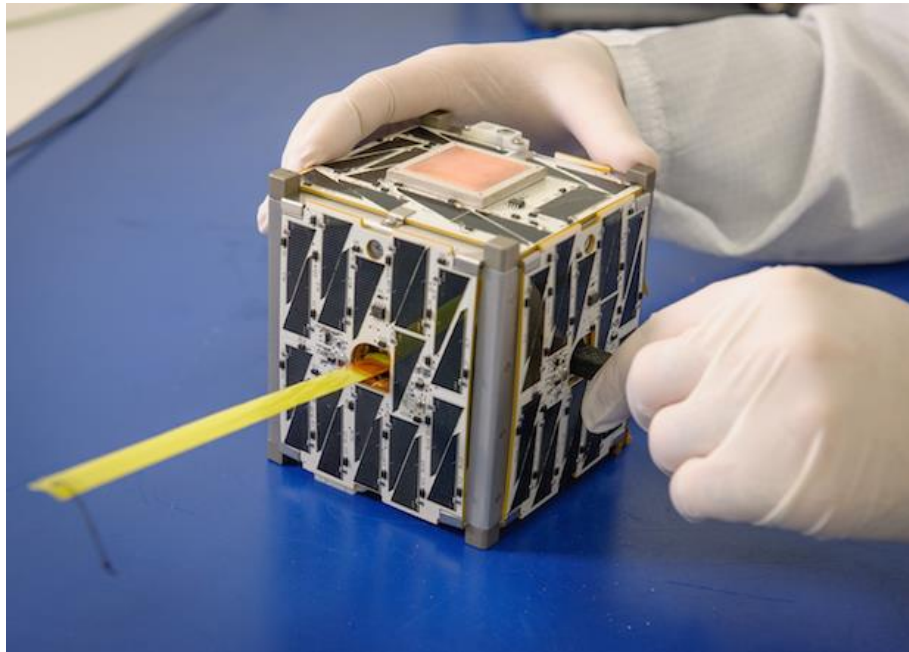


Figure 3: CubeSat 1U [8]

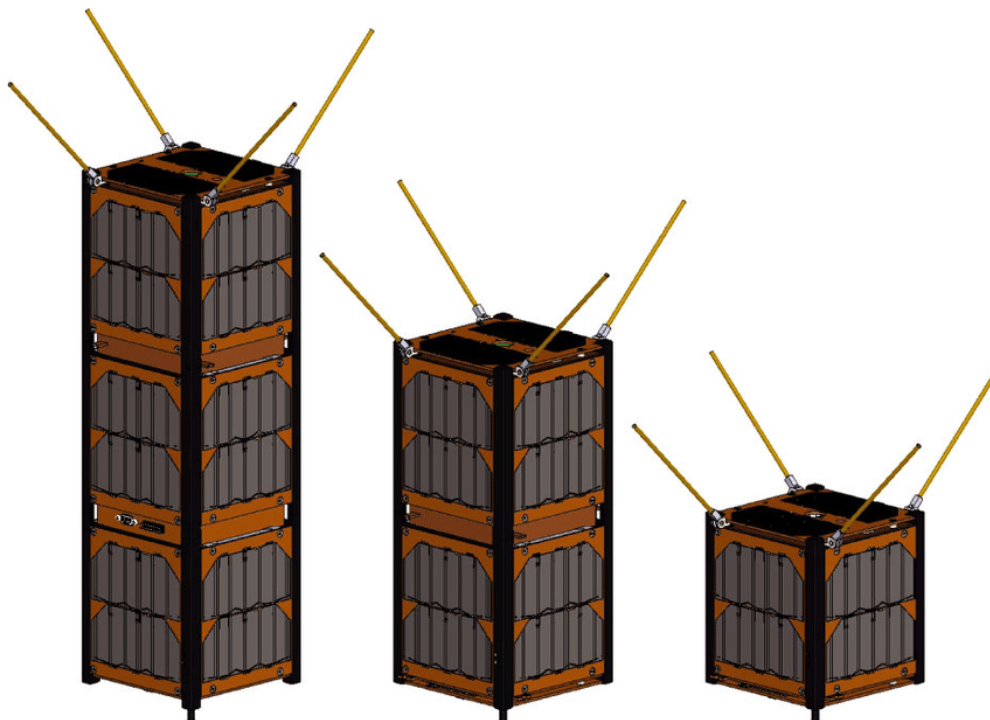


Figure 4: 3U, 2U and 1U CubeSats [9]

Here are some examples of commercial products specifically designed for CubeSats:

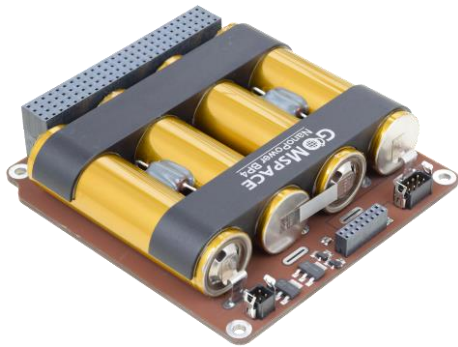


Figure 5: Standard battery module for CubeSat [10]



Figure 6: 1U CubeSat structure [11]

The whole characteristics that a CubeSat must have are defined in [9].

#### 4.4. Satellite subsystems

Satellites usually present the same subsystems in order to perform its functions and survive in space for the duration of its mission (small scheme on figure 10).

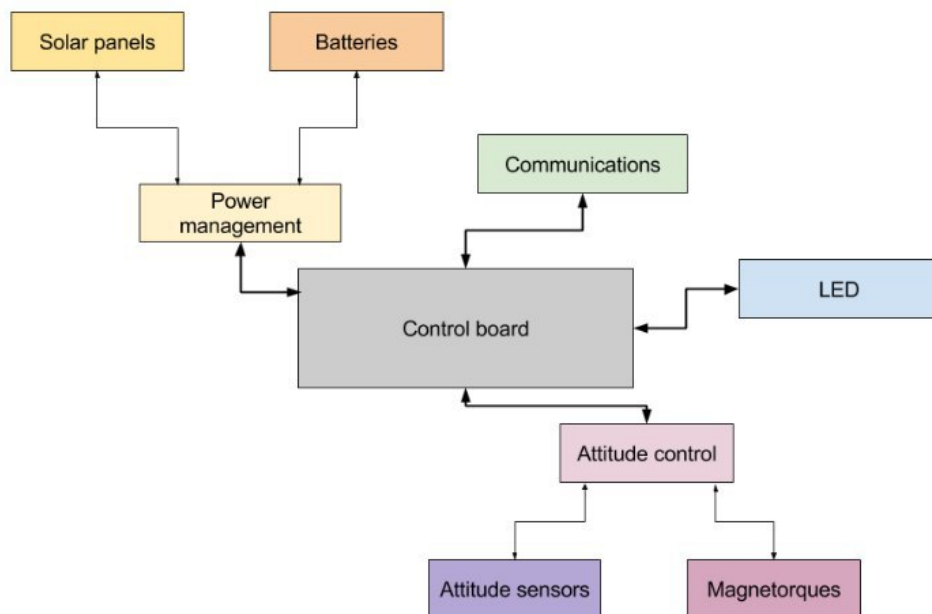





Figure 7: Teidesat CubeSat scheme [8]

Page: 13 of 40	Thermal analysis for the Teidesat / Alisio CubeSat			
----------------	--	--	---	---

#### ·Payload

Is the mission main system, the scientific instruments that will perform the mission, in case of the Teidesat project it is a pack of Leds and the controller that will control the pulses of light in order to transmit a message.

In case of ALISIO mission, the payload will be a SWIR camera that will operate in LEO, for at least one year, obtaining images of the Canary Islands with a wide swath (>150 km) and a moderate GRD (< 500 m).

Some of the applications of SWIR images obtained are shown below:

- Measure of desertification, thanks to the sensitivity of the SWIR spectrum to moisture.
- Track and characterization of clouds.
- Detection of hot spots in fires, thanks to the capability of the SWIR region to detect thermal emission mainly between 200 and 800°C.
- Detection of human impact in ocean, thanks to the reflectance of synthetic materials in SWIR range.
- Flooding control. A constellation of satellites with enough resolution and a short revisit time would allow evaluating the impact of flooding events.

#### · ACDS subsystem

This subsystem is responsible for controlling (Attitude Control System, ACS) and determining (Attitude Determination System, ADS) the orientation of our satellite. It mainly depends on the payload necessities of the satellite.[10]

#### · Communication subsystem

A critical usual feature in mission goals and functionality as a satellite is to be able to stablish communication with a ground station, so satellites usually have a radio that can communicate with the ground.



- Power Subsystem

To perform its function and power up all the subsystems in space the satellite needs electrical energy, so satellites always have a way to collect energy (solar panels) and another way to store it (batteries).

- On board computer

This subsystem exists in order to control satellite functions and handling the data.

- Structure

This subsystem is the physical part that contains all the others, in the case of the CubeSat this has very specific measures according to the CubeSat standard considered (figure 8).

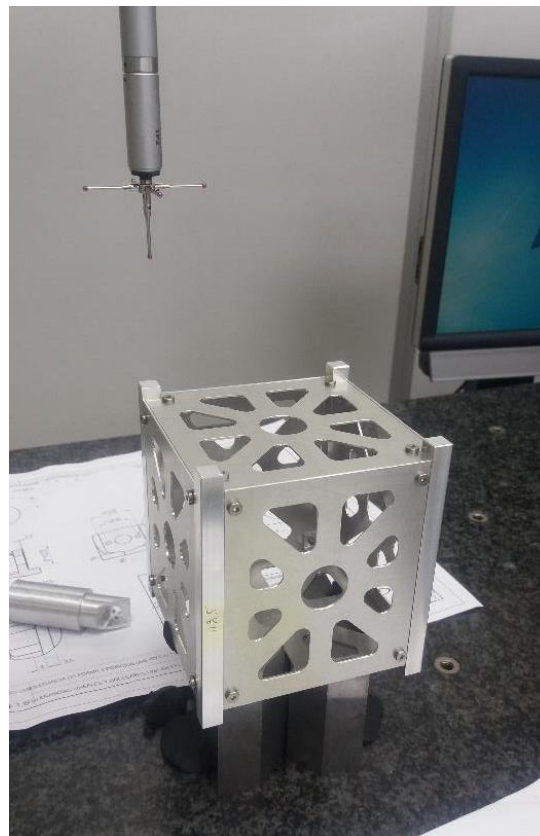


Figure 8: External structure of Teidesat satellite[11]



· Thermal Subsystem

The objective of the thermal design is to bring temperatures inside the spacecraft into a range where the components can safely operate, and to ensure that internally generated heat from the spacecraft components is conducted or radiated out. Typical component temperature operating ranges are:

Component	Typical temperature operating range °C
Electronics	-20 to +40
Special electronics (like Reaction wheels)	0 to 35
Solar Panels	-100 to +100

*Table 1: Temperatures of operation [12]*

The heat sources seen by a spacecraft are direct radiation by the sun, Earth-reflected radiation of the Sun (Albedo) and outgoing long wave Earth radiation. The sun incident power varies between 1322 and 1414 W/m<sup>2</sup>, with an average value of 1367 W/m<sup>2</sup> [12].

The Earth-reflected power (Albedo) and Long Wave outgoing radiation from Earth vary with altitude and position around the Earth. Albedo radiation is mostly in the visible range and has a mean reflectance of 0.3, meaning that 0.3 times the incident sun energy is reflected from Earth omnidirectionally. The reflection coefficient is less 0.25 near the Equator and about 0.7 toward the Poles.[12]

The challenge faced by most spacecraft designs is to get rid of the large amount of incident heat [12] and as there is no air or any fluid in space, it is not possible to transfer heat via convection. Then, all the heat received or rejected goes via radiation, and inside the satellite, heat transfer goes via conduction and radiation.

Absorption and radiation of heat can be altered by:

- Surface Finishes (white paint will reduce the temperature; black paint will increase the temperature)
- Metallic conduction from hot parts of the spacecraft to cold parts so it could radiate heat into space
- Heat pipes that can increase thermal conduction from one point to another





- Heaters (to increase the temperature of components that are too cold – like batteries)
- Louvers that can open or close surfaces and can change their absorptivity or emissivity
- MLI (Multi-Layer Insulation) to protect a wrapped volume by reducing absorbed radiation
- Thermoelectric Coolers (to spot cool electronics parts)
- Placing heat-generating components where it is easy to get rid of heat


The goal is to design this subsystem in order to keep the temperature of each component into its range of correct functioning; for all components, the average values would be  $0^{\circ}$ – $40^{\circ}$  °C [12]. More specifically for small spacecrafts (like CubeSats) this subsystems is required to have more passive solutions than actives ones (small satellite means smaller energy available).

These subsystems will be the one developed in this project, it will be the first version, and many iterations will be done in the future.

## 5. Solution analysis

In steady state, the heat absorbed from the Sun, Albedo and Earth IR, plus the heat generated in the spacecraft equals the heat radiated out for some spacecraft temperature. The thermal design process is to vary surface finishes and radiators to achieve this balance at the desired spacecraft temperature. The design process consists of the following steps:

1. Flow down the thermal requirements from component thermal specifications (to determine the acceptable spacecraft and component temperature ranges). As no final inner components are decided in the spacecraft the temperature goal is set in  $0 - 40^{\circ}$ C in the whole spacecraft)
2. Assess the solar flux, Albedo and Earth IR radiation incident on the spacecraft in its orbit and compute the orbit average heat on each of the spacecraft outside surfaces. The environment depends on the Beta angle. Assess the range of Beta over the mission life of the spacecraft. For the firsts approaches medium values of the solar flux the albedo and the earth IR will be considered, and the beta degree will be  $0^{\circ}$ .
3. Compute the heat absorbed by the spacecraft surfaces.
4. Determine the heat generated by the spacecraft electronics. As the electronics are not decided a usual value will be used for the calculations.

Page: 17 of 40	Thermal analysis for the Teidesat / Alisio CubeSat	
----------------	--	---

5. The sum of the heat from steps 3 and 4 is the heat that has to be rejected for steady state. Iterate radiator and surface finishes to reject that much heat.
6. Construct a thermal model, including locations of its heat generating components.
7. Compute spacecraft temperatures as a function of time.
8. . Apply techniques to bring these temperatures within component specifications. These techniques include:
  - a. Applying paint or other surface finishes to reduce heat absorption or increase heat radiation.
  - b. Apply heaters to increase temperatures of cold components (such as batteries).
  - c. Use metallic or other heat conductors to take heat from hot components to points from where heat can be radiated out to space
  - d. When the spacecraft is completed, conduct thermal vacuum tests to determine the actual spacecraft and component temperatures as a function of time and in the steady state
  - e. Correlate the thermal model to bring it in conformity with actual measurements obtained during test
  - f. Generate adjusted model predictions of the spacecraft thermal behaviour in all conditions relevant to mission life in orbit. [12]

This is the whole process that will be followed in future stages of the mission, for this document only a first approach is developed.

In order to predict the temperature of the spacecraft in the most critical moments, different approximations will be performed. First ones shall have less accuracy and the later ones shall add more accuracy, ending in a case where a real surface is considered and both the hottest and the coldest cases are analysed (the environment considered for this is explained in the Annex 3: 6. Space environment) . The table 2 shows what conditions will be considered on each case.

Approximation Conditions	1. Case plate	2. Sphere case	3. Cube case	4. Case all heat sources	5. Case considering real surface	6. Cold case
<b>State</b>	Stationary	Stationary	Stationary	Stationary	Stationary	Stationary
<b>Black body</b>	Yes	No	No	No	No	No
<b>Surface</b>	Ideal	Al/black & white paints	Al/black & white paints	Commercial paints	Solar panels & commercial paints	Solar panels & commercial paints
<b>Sun heat</b>	Yes	Yes	Yes	Yes	Yes	No
<b>Albedo heat</b>	No	No	No	Yes	Yes	No
<b>Earth IR heat flux</b>	No	No	No	Yes	Yes	Yes
<b>Internal Heat</b>	No	No	No	Yes	Yes	Yes
<b>Shape</b>	Plate	Sphere	Cube 1U	Cube 1U	Cube 1U	Cube 1U
<b>Solid/shell</b>	Surface	Solid	Solid	Solid	Solid	Solid

Table 2: Conditions for each case

For this analysis, solution will be approached in different ways:




First one will be an approximation considering that the shape of the spacecraft is just a plate.

### 5.1. Case plate

The temperature of a body in space only considering average sun at normal incidence (at 1AU) is given by[12]:

$$T(K) = \left( \frac{S^* \left( \frac{\alpha}{\epsilon} \right) \left( \frac{A_i}{A_r} \right)}{\sigma} \right)^{\frac{1}{4}} \quad (ec. 1)$$

- $S^*$ : Sun radiance (1367W/m<sup>2</sup> as a mean value; usually it varies a 7% annually)
- $\alpha, \epsilon$ : absorptivity and emissivity
- $A_i$ : Area of the surface of sun incidence normal to the sun

Page: 19 of 40	Thermal analysis for the Teidesat / Alisio CubeSat			
----------------	--	--	---	---

- $A_r$ : Area of the surface radiating to space
- $\sigma$ : Stefan Boltzmann constant ( $5,67 \cdot 10^{-8} \text{ W/m}^2/\text{K}^4$ )

Black body condition will be applied (is an idealized physical body that absorbs all incident electromagnetic radiation, regardless of frequency or angle of incidence. It also emits radiation). Both emissivity and absorptivity are equal to one when this condition is applied. (more info in Annex 3: Theoretical context)

Considering a plate of absorptivity and emissivity equal to 1,0 in a plate  $1 \text{ m}^2$  plate we have:

$$T(K) = \left( \frac{1367 \text{ W/m}^2 \left( \frac{1,0}{1,0} \right) \left( \frac{1,0}{1,0} \right)}{5,67 \cdot 10^{-8} \text{ W/m}^2/\text{K}^4} \right)^{\frac{1}{4}} = 394 \text{ K} = 120,9^\circ\text{C}$$

This temperature is above the survival temperature of most components in a satellite, note that here a bigger surface is being considered and the material denomination ( $\alpha, \epsilon$ ) is not real. Also, neither the Albedo or the Earth IR are being considered (Annex 3: 6. Space environment)

## 5.2. Sphere case

Considering a sphere, which has  $A_i/A_r = \pi r^2 / 4\pi r^2$  [13], and considering 3 different surfaces:

- Aluminium (6061-T6)-Polished Metal surface: this material is one of the aluminium alloys most widely used in Cubesats, it is usually covered by paint or treated because its low absorptivity and emissivity.

- Paint white AZ-93: is an inorganic white thermal control paint developed for use on spacecraft / satellite surfaces exposed to the deleterious effects of the space environment. Application of AZ-93 creates a nonspecular white coating that provides superior thermal control / protection by allowing only 14-16% of the solar radiation impinging on the spacecraft external surface to be absorbed through to the interior systems while emitting 89-93% of the internal heat generated to the cold vacuum of space [14].

- Paint Aeroglaze Z306: These moisture cured polyurethanes provide a matt black nish with extreme durability, mar resistance, cleanability and resistance to environmental degradation. Many scientific evaluations of Z306 have established its properties for the high absorption of wavelengths in the visible spectrum (low reflectance), combined with low emissivity in the infra-red spectrum. These properties ensure maximum absorption of stray light & minimum scatter combined with minimum emission of heat which can disturb the light path [15].

If the sphere surface is Aluminium (6061-T6)-Polished Metal; Solar absorptivity  $\alpha/\epsilon=0,031/0,039$  [16]:

$$T(K) = \left( \frac{1367W/m^2 \left( \frac{0,031}{0,039} \right) \left( \frac{1}{4} \right)}{5,67 * 10^{-8} W/m^2/K^4} \right)^{\frac{1}{4}} = 263,09 K = -10,05^{\circ}C$$

If the sphere is painted with Z93 white,  $\alpha/\epsilon=0,17/0,92$

$$T(K) = \left( \frac{1367W/m^2 \left( \frac{0,17}{0,92} \right) \left( \frac{1}{4} \right)}{5,67 * 10^{-8} W/m^2/K^4} \right)^{\frac{1}{4}} = 182,68 K = -90,46^{\circ}C$$

For a sphere painted with Z306 black,  $\alpha/\epsilon=0,921/0,89$

$$T(K) = \left( \frac{1367W/m^2 \left( \frac{0,921}{0,89} \right) \left( \frac{1}{4} \right)}{5,67 * 10^{-8} W/m^2/K^4} \right)^{\frac{1}{4}} = 281,027 K = 7,8^{\circ}C$$

### 5.3. Cube case

Considering now a CubeSat 1U made of aluminium 6061-T6 and the satellite in line with the sun we have that one face is exposed to the Sun radiation heat ( $A_i=10\text{ cm}^2$ ) and all the surface is emitting heat ( $A_r=60\text{ cm}^2$ ). The three previous surfaces will be considered:

If the surface is Aluminium (6061-T6)-Polished Metal;  $\alpha/\epsilon=0,031/0,039$  [16]:

$$T(K) = \left( \frac{1367 W/m^2 \left( \frac{0,031}{0,039} \right) \left( \frac{10}{60} \right)}{5,67 * 10^{-8} W/m^2/K^4} \right)^{\frac{1}{4}} = 237,72 K = -35,42 ^\circ C$$

If the sphere is painted with Z93 white,  $\alpha/\epsilon = 0,17/0,92$

$$T(K) = \left( \frac{1367 W/m^2 \left( \frac{0,17}{0,92} \right) \left( \frac{1}{6} \right)}{5,67 * 10^{-8} W/m^2/K^4} \right)^{\frac{1}{4}} = 165,07 K = -108,07 ^\circ C$$

For a sphere painted with Z306 black,  $\alpha/\epsilon = 0,921/0,89$

$$T(K) = \left( \frac{1367 W/m^2 \left( \frac{0,921}{0,89} \right) \left( \frac{1}{6} \right)}{5,67 * 10^{-8} W/m^2/K^4} \right)^{\frac{1}{4}} = 253,94 K = -19,21 ^\circ C$$

This means that in the hotter case with this surface finish and only considering the sun as a heat source the temperature will be below the surviving temperature of the electronics of the spacecraft (taking into account that this temperature is only on the case and only heat incidence in one face is being considered).

Although the total area is approximately the same the sphere case this temperature is 20°C lower, this is caused by the position related so sun considered, only one of the six faces is directed towards the sun, which is only 1/6 of the total area. However, if we consider that the sun is directed to a vertex of the cube, and so heating three faces, we have that:

If the surface is Aluminium (6061-T6)-Polished Metal;  $\alpha/\epsilon = 0,031/0,039$  [16]

$$T(K) = \left( \frac{1367 W/m^2 \left( \frac{0,031}{0,039} \right) \left( \frac{30}{60} \right)}{5,67 * 10^{-8} W/m^2/K^4} \right)^{\frac{1}{4}} = 312,87 K = 39,72 ^\circ C$$

If the sphere is painted with Z93 white,  $\alpha/\epsilon = 0,17/0,92$

$$T(K) = \left( \frac{1367 W/m^2 \left( \frac{0,17}{0,92} \right) \left( \frac{3}{6} \right)}{5,67 * 10^{-8} W/m^2/K^4} \right)^{\frac{1}{4}} = 217,24 K = -55,90 ^\circ C$$

For a sphere painted with Z306 black,  $\alpha/\epsilon = 0,921/0,89$

$$T(K) = \left( \frac{1367 W/m^2 \left( \frac{0,921}{0,89} \right) \left( \frac{3}{6} \right)}{5,67 * 10^{-8} W/m^2/K^4} \right)^{\frac{1}{4}} = 334,19 K = 61,04 \text{ } ^\circ C$$

Case	Aluminium polished	Z93 white	Z306 black
Sphere	-10 °C	-90 °C	7 °C
Cube one face	-35 °C	-108 °C	-19 °C
Cube 3 faces*	39 °C	-55 °C	61 °C

Table 3: Results comparison

\*As the angle of incidence between the surface and the sunlight is not being considered, an error exists within this calculation, although it will be corrected in future cases in this document.

When comparing temperatures obtained it is observed that the position of the satellite related to the sun is highly important because the amount of heat flux absorbed depends on it, in further calculations this will be considered as well as how the sun intensity changes with the angle of incidence.

However, in this table below we can see the temperature obtained in different cases with different commercial paints, but in all of them only once **face exposed to the sun is being considered**.



Coating	Solar absorptivity	Infrared emissivity	Area receiving radiation	Area emitting radiation	Temperature		Shape	Type of coat
					K	°C		
-	$\alpha_\lambda$	$\epsilon_{IR}$	$A_i$	$A_r$	T		-	-
-	-	-	cm <sup>2</sup>	cm <sup>2</sup>	K	°C	-	-
Al 6061 T6	0,031	0,039	10	60	237,729361	-35,420639	1U	Polished metal
Anodize black	0,88	0,88	10	60	251,7726502	-21,3773498	1U	Black coating
Velestat black plastic	0,96	0,85	10	60	259,5503556	-13,5996444	1U	Black coating
Varium sulphate with white polyvinyl alcohol	0,06	0,88	10	60	128,6547117	-144,495288	1U	White coating
Hughson white paint Z255	0,25	0,89	10	60	183,2930727	-89,8569273	1U	White coating
Blue anodized titanium foil	0,7	0,13	10	60	383,5281303	110,37813	1U	White coating
Gold	0,48	0,82	10	60	220,2243808	-52,9256192	1U	Anodized aluminum
Ethanol C black	0,97	0,77	10	60	266,7342615	-6,41573848	1U	Anodized aluminum

Table 4: Temperature of a CubeSat with different coatings [17]



Values of the coatings are to be found in [17]

This data reflects a first estimation of how materials of the surface affect to the temperature of the spacecraft, although it is important to keep in mind that position along the orbit is not being considered, neither are Albedo and Earth IR, and the satellite is being considered a solid mass in one stationary position (closest to the Sun) .

#### 5.4. All heat sources case

In order to obtain the stationary temperature considering extreme positions in orbit, and considering Earth infrared emission, albedo, internal heat, and heat rejection, we summarize all the heat flows (considering the a satellite as a solid body with the same temperature all across it) [18]:

$$Q_{in} - Q_{out} + Q_{generated} = 0 \text{ (ec. 2)}$$

Being then:

$$Q_{in} = Q_{solar} + Q_{albedo} + Q_{earth IR}$$

$$Q_{solar} = S^* * A_i * \alpha * \cos(\gamma) \text{ (ec. 3)}$$

$$Q_{albedo} = a * S^* * A_e * \alpha * vf \text{ (ec. 4)}$$

$$Q_{earth IR} = G_{IR} * A_e * vf \text{ (ec. 5)}$$

$$Q_{out} = A_r * \varepsilon * \sigma * T^4 \text{ (ec. 6)}$$

Where:

$Q_{in}$	Heat incidence to satellite surface (W)	$G_{IR}$	Earth IR (W/m <sup>2</sup> )
$Q_{out}$	Emitted heat from the satellite surface (W)	$A_i$	Area pointing toward the sun (m <sup>2</sup> )
$Q_{Generated}$	Radiation generated by the onboard electronics (W)	$A_e$	Area pointing towards the earth (m <sup>2</sup> )
$S^*$	Solar constant (W/m <sup>2</sup> )	$A_r$	Area pointing towards the space
$a$	Albedo factor	$Vf$	View factor
$\epsilon$	The emissivity factor	$\alpha$	Absorptivity of each material
$\gamma$	Angle between an imaginary ray linking the sun and the satellite	$\sigma$	Stefan–Boltzmann constant (W/m <sup>2</sup> /K <sup>4</sup> )

Table 5: Parameters for the equation

The heat generated inside the satellite depends on the payload and the subsystems that are inside it, in Teidesat case, the hotter case would be when the payload its working, due to its high consume of power, we can consider that the heat dissipated will be **around 5 W**.

Note that the Q received by the Sun does not exist during eclipses, we are analysing the hottest case possible here (payload on and maximum Sun incidence, which is the closes distance, see figure 9).

$$(S^* * A_i * \alpha * \cos(\gamma)) + (a * S^* * A_e * \alpha * vf) + (G_{IR} * A_e * vf) - (A_r * \epsilon * \sigma * T^4) + 5 = 0 \text{ (ec. 7)}$$

Temperature is:

$$T(K) = \left( \frac{(S^* * A_i * \alpha * \cos(\gamma)) + (a * S^* * A_e * \alpha * vf) + (G_{IR} * A_e * vf) + 5}{A_r * \epsilon * \sigma} \right)^{\frac{1}{4}} \text{ (ec. 7)}$$

According to [18] the values of  $\gamma$  are  $[\pi/2, 3\pi/4, \pi/4]$

And the vf ones [0,24; 0,6; 0,02]

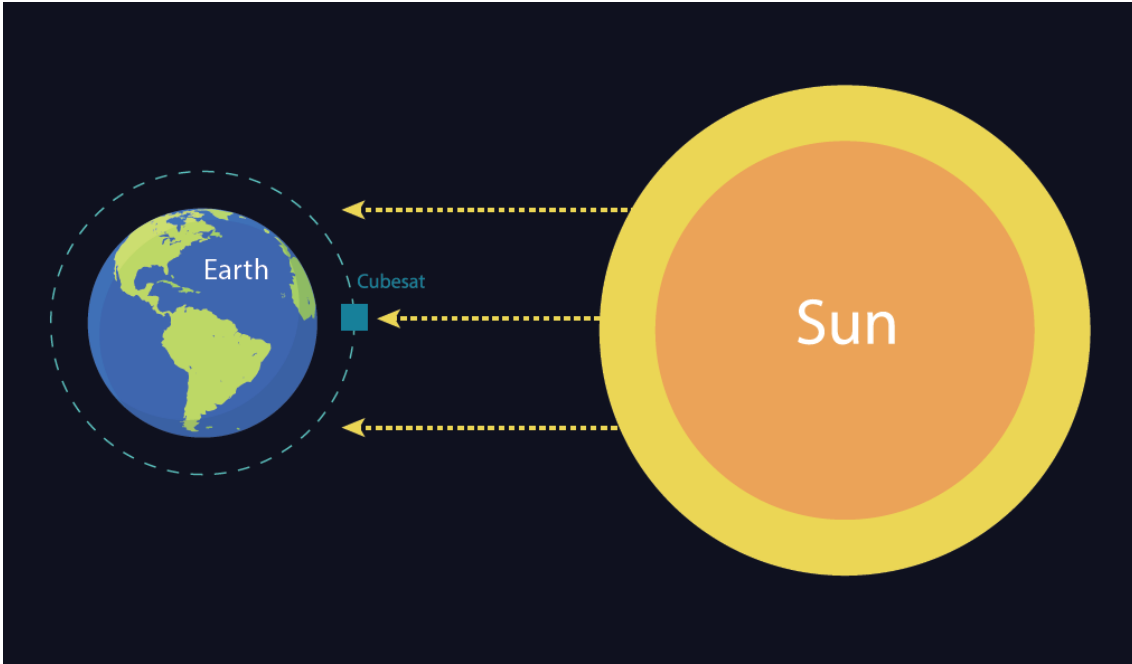


Figure 9: Extreme position of the satellite illustrated by Eduardo Puyol Correa

Terms of this calculation (table 6):

- The  $\cos(\gamma)$  of this angle is a calculation of the visibility factor Sun-satellite
- Albedo is the percentage of sun radiation reflected in the atmosphere, and it changes depending on the part of earth that the satellite is orbiting, its maximum value is 35%
- As we are analysing the hotter case possible the values of  $\nu_f$  and  $\gamma$  that contribute more to the heat will be selected, which are 0,6 and  $\pi/4$ .

<b>S*</b>	<b>1367</b>	<b>W/m<sup>2</sup></b>
<b>a</b>	<b>0,35</b>	<b>%</b>
<b><math>\alpha</math></b>	<b>*</b>	<b>-</b>
<b>Ai</b>	<b>0,1</b>	<b>m<sup>2</sup></b>
<b>Ae</b>	<b>0,1</b>	<b>m<sup>2</sup></b>
<b>GIR</b>	<b>221</b>	<b>W/ m<sup>2</sup></b>
<b>Q generated</b>	<b>5</b>	<b>W/ m<sup>2</sup></b>
<b>Ar</b>	<b>0,6</b>	<b>m<sup>2</sup></b>
<b><math>\epsilon</math></b>	<b>*</b>	<b>-</b>
<b><math>\sigma</math></b>	<b>5,67E-08</b>	<b>W/ m<sup>2</sup>/K<sup>4</sup></b>
<b><math>\nu_f</math></b>	<b>0,6</b>	<b>-</b>
<b><math>\cos(\gamma)</math></b>	<b>0,707106</b>	<b>-</b>

Table 6: Data for the equation



Different material for the surface will be evaluated (one face facing the sun):

$\alpha_\lambda$	$\epsilon_{IR}$	Coating	Type	T(K)	T(°C)
0,031	0,039	Al 6061 T6	Polished metal	388,2777815	115,1277815
0,88	0,88	Anodize black	Black coating	330,2106587	57,06065874
0,96	0,85	Velestat black plastic	Black coating	340,0470527	66,89705267
0,06	0,88	Varium sulphate with white polyvinyl alcohol	White coating	192,7040789	-80,4459211
0,25	0,89	Hughson white paint Z255	White coating	247,8156173	-25,3343827
0,7	0,13	Blue anodized titanium foil	White coating	504,6643688	231,5143688
0,48	0,82	Gold	Anodized aluminum	291,8723835	18,72238354
0,97	0,77	Ethanol C black	Anodized aluminum	349,4164246	76,26642461

Table 7: Temperature of a CubeSat for different material

A small classification on optical surface of the material according to its type is presented here (figure 10):

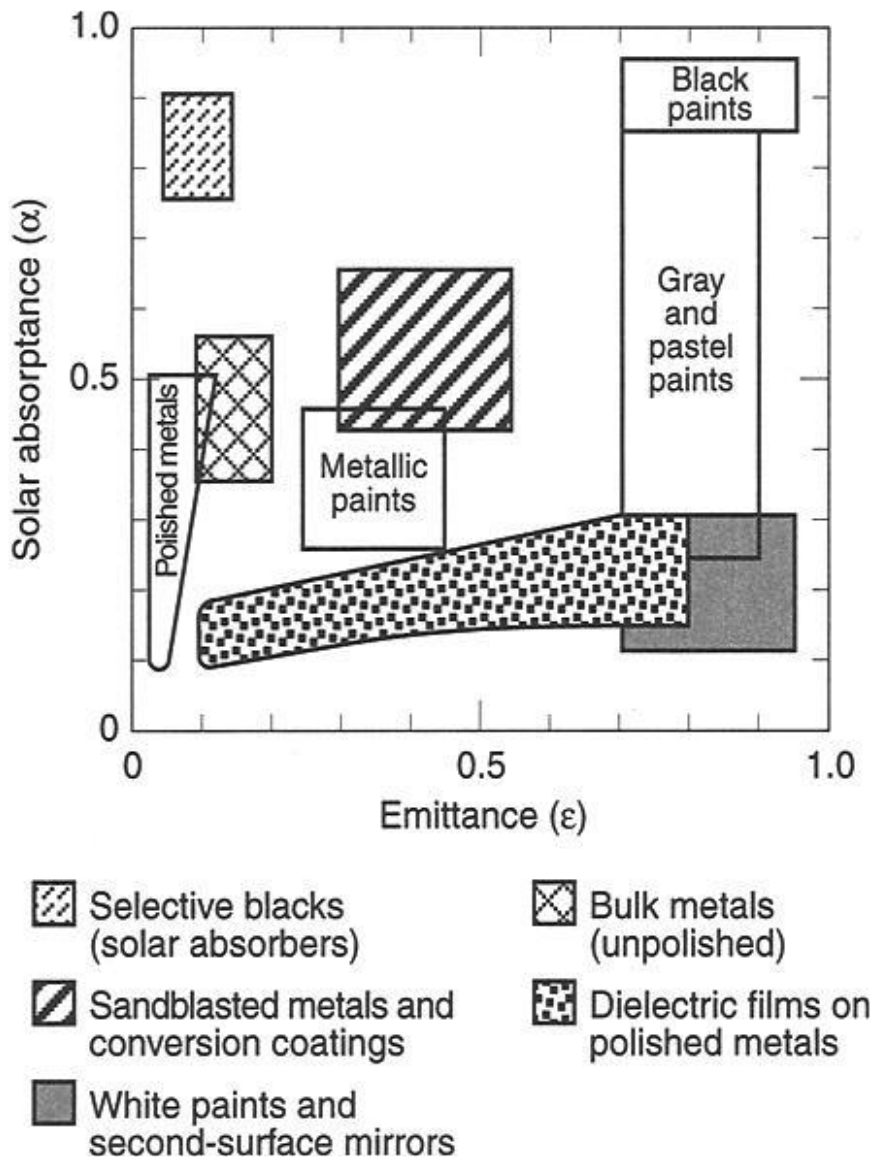


Figure 10: Surface properties by type of finish [19]

### 5.5. Case considering real surface

Going one step forward we are going to have a real face of CubeSat (with solar cells) and more real values of absorptivity and emissivity [19]

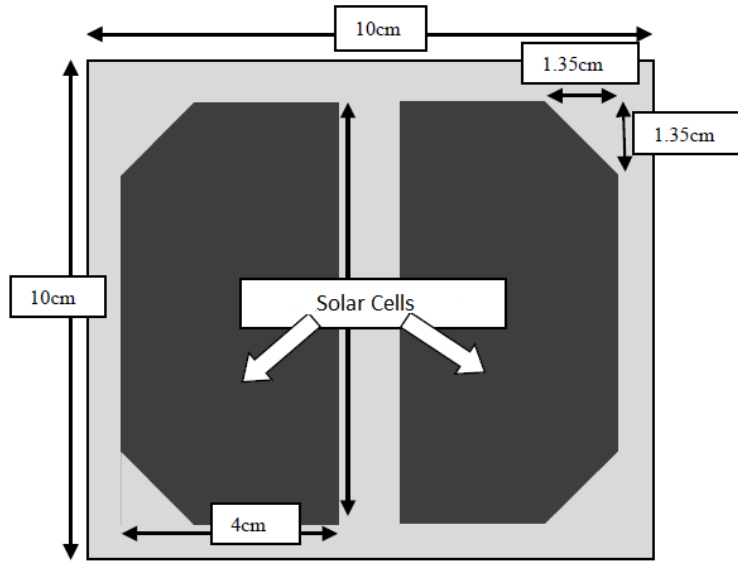


Figure 11: CubeSat face distribution

Which is approximately a 40% of or the selected surface and a 60% of solar panel, so absorptivity:

$$\alpha = 0,4 * \alpha_{surface} + 0,6 * \alpha_{Solar Cell} \text{ (ec. 8)}$$

And so goes emissivity:

$$\varepsilon = 0,4 * \varepsilon_{surface} + 0,6 * \varepsilon_{Solar Cell} \text{ (ec. 9)}$$

Table 8 presents values of solar cells for different missions

Name	$\alpha_{Solar Cell}$	$\varepsilon_{IR}$
AE	0,78	0,82
AMSAT	0,82	0,85
ATN Black	0,77	0,80
ATN blue	0,86	0,85
GOES	0,91	0,81
IUE	0,77	0,81
SSS	0,79	0,82

Table 8: Values for solar cells used in other space missions [17]

Some cells values have been selected for testing; the values are from actual spacecrafts.

As normal absorptive values are high for solar cells, a material with high emissivity and/or low absorptivity should be chosen.

In table 9 different combinations will be seen (go to Annex 1 for further information)

Solar cell	Surface	T°C
AE	Anodize black	54,9949509
IUE	Gold surface	40,8555414
SSS	Alzac A-2	29,8145545
ATN Black	GSFC SiOx Al <sub>2</sub> O <sub>3</sub> -Ag	26,5113157
IUE	2mil Aclar film	30,5504378

*Table 9: Temperatures for CubeSat with different combinations of surfaces*

As is to be seen on the results, many materials combined with different solar cells do give an appropriate value for temperatures in hot case, in order to pick one the cold case will be analysed first, and each of the material (for both solar cells and coating) will be studied,

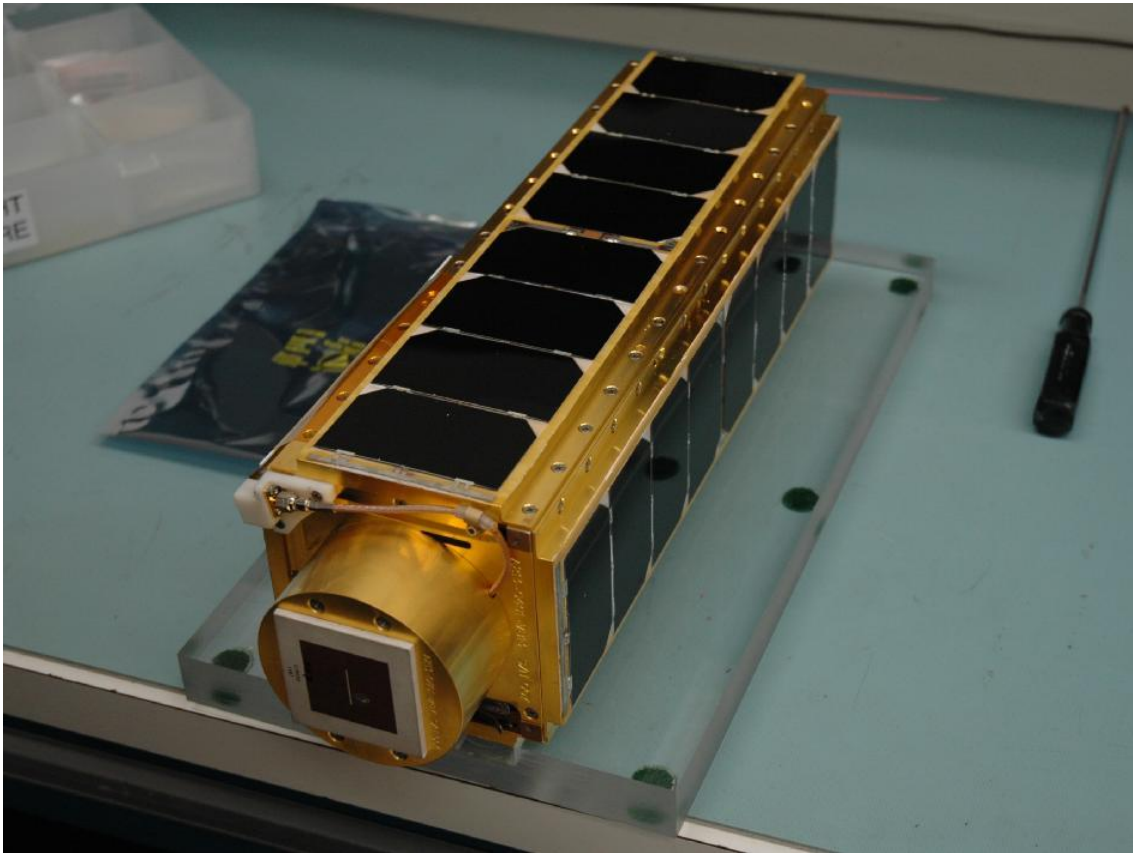


Figure 12: Pharmasat [21]

## 5.6. Cold case

Considering the extreme coldest case possible (eclipse), we have that there is not any solar incidence or albedo, only inner Heat generation and Earth IR heat fluxes

$$Q_{in} - Q_{out} + Q_{generated} = 0 \text{ (ec. 2)}$$

Being then:

$$Q_{in} = Q_{solar} + Q_{albedo} + Q_{earth IR}$$

$$Q_{solar} = 0 \text{ (ec. 3)}$$

$$Q_{albedo} = 0 \text{ (ec. 4)}$$

$$Q_{earth IR} = G_{IR} * A_e * v_f \text{ (ec. 5)}$$



$$Q_{out} = A_r * \epsilon * \sigma * T^4 \text{ (ec. 6)}$$

So:

$$G_{IR} * A_e * vf = A_r * \epsilon * \sigma * T^4 \text{ (ec. 7)}$$

$$T(K) = \left( \frac{(G_{IR} * A_e * vf) + 5}{A_r * \epsilon * \sigma} \right)^{\frac{1}{4}} \text{ (ec. 7)}$$

<b>S*</b>	<b>0</b>	<b>W/m<sup>2</sup></b>
<b>a</b>	<b>0,35</b>	<b>%</b>
<b>α</b>	<b>*</b>	<b>-</b>
<b>Ai</b>	<b>0,1</b>	<b>m<sup>2</sup></b>
<b>Ae</b>	<b>0,1</b>	<b>m<sup>2</sup></b>
<b>GIR</b>	<b>221</b>	<b>W/ m<sup>2</sup></b>
<b>Q generated</b>	<b>5</b>	<b>W/ m<sup>2</sup></b>
<b>Ar</b>	<b>0,6</b>	<b>m<sup>2</sup></b>
<b>ε</b>	<b>*</b>	<b>-</b>
<b>σ</b>	<b>5,67E-08</b>	<b>W/ m<sup>2</sup>/K<sup>4</sup></b>
<b>vf</b>	<b>0,1</b>	<b>-</b>
<b>cos(y)</b>	<b>0,707106</b>	<b>-</b>

Table 10: Data for the equation

$$T(K) = \left( \frac{221 * 0,1 * 0,1 + 5}{0,6 * \epsilon * 5,67 * 10^{-8}} \right)^{\frac{1}{4}}$$

Now for any material chosen the temperature will be lower than our minimum 0°C, but this calculation is the temperature of the surface of a solid CubeSat, case which is not real.

If the surface was completely covered in blue anodized titanium foil (for example) temperature in cold case is:

$$T(K) = \left( \frac{221 * 0,1 * 0,1 + 5}{0,6 * 0,13 * 5,67 * 10^{-8}} \right)^{\frac{1}{4}} = 253,48K = -19,66°C$$

As was previously done, now we will do the same but supposing a 60% of the surface of each face covered with solar panels, the ones with lowest emissivity will be chosen (complete table at annex 1)

Solar cell	Surface	Temperature [°C]
ATN Black	Blue anodized titanium foil	-94,9270172
ATN Black	gold	-112,607961

Table 11: Temperatures for CubeSat with different combinations of surfaces

### 5.7. ESATAN-TMS results

As the complexity of a deeper calculation is dependent of many variables thermal analysis is usually performed on different software, ESATAN-TMS is one of those software ITP Engines UK is kindly sponsoring Teidesat with the software license for the analysis and simulation software ESATAN-TMS.



Both Teidesat (CubeSat 1U) and Alisio (CubeSat 3U) will be studied (detailed in Annex2: ESATAN-TMS).

### Teidesat case

Generating a model cube shaped completely made of Aluminum T6-6061; we obtain these temperatures along the orbit

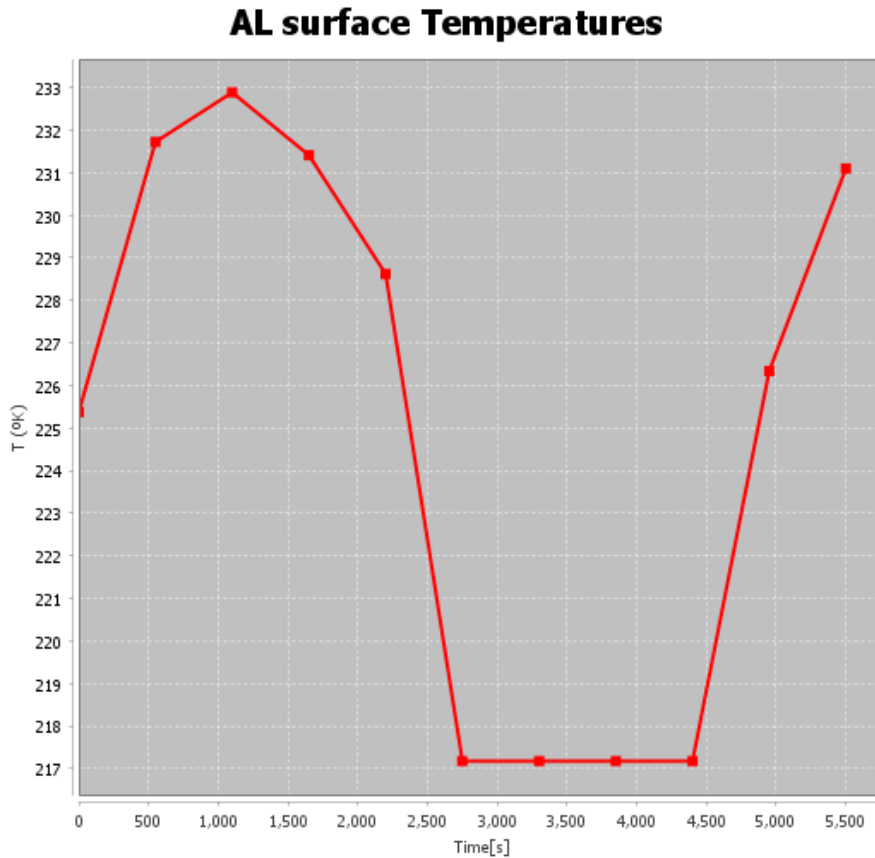


Figure 13: Temperature-time graph in one orbit

Comparing it to the theoretical calculations seen before maximum temperature is quite similar, being the software one 232 °K and the calculated 237 °K (4.3. Cube Case). However, this theoretical case is not considering all heat sources, in (4.4) temperature with this surface is 388 °K.



If the surface is anodized black aluminium, we have:

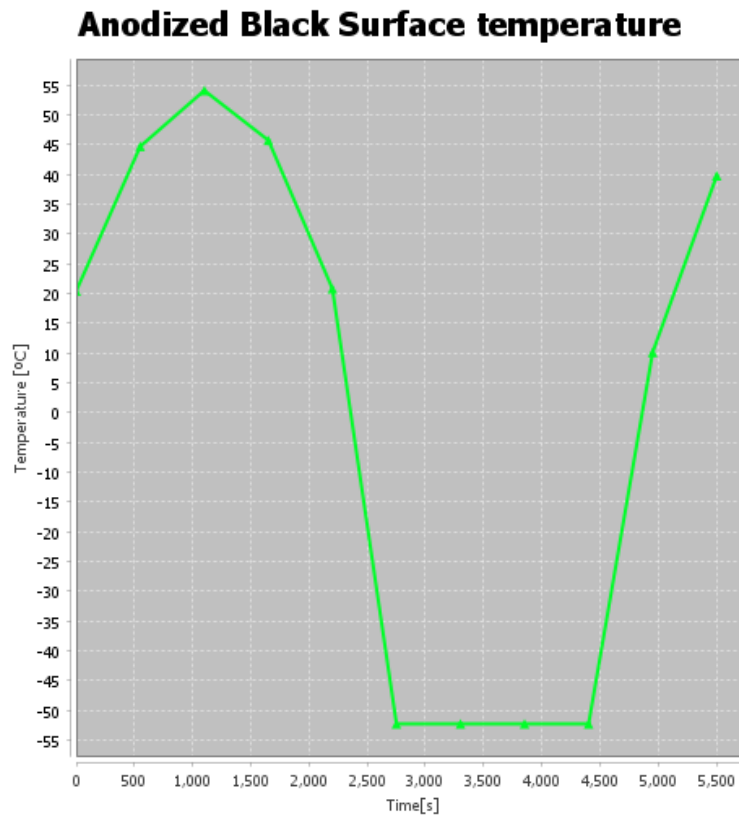


Figure 14: Temperature-time graph in one orbit

Comparing it to the theoretical calculations we observe that maximum temperature is 55°C in the software and 57°C in the calculations performed (4.4. All heat sources case)

For these simulations, the thickness of the satellite walls is being neglected, as well as the inner components and its connections, making them not very precise.

For the final purpose material to Teidesat satellite in this document a surface with mesh, real wall thickness (2mm) and absorptivity and emissivity of the surface will be estimated considering the optical set as the mean value of having solar panels ATN black and anodize black in all surfaces (mean value  $\alpha/\epsilon=0,814/0,832$ ); heat from the payload has been added, but no inner structure is yet considered.

With a right ascension angle of  $-30^\circ$  (high sun exposure along orbit) we obtain:

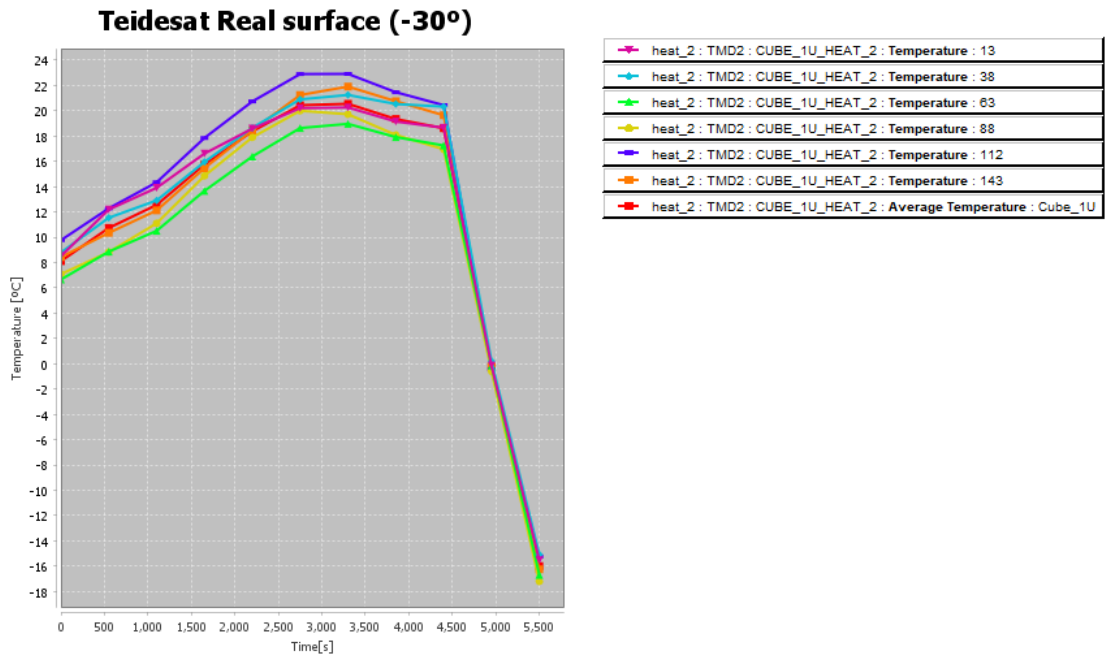


Figure 15: Teidesat temperature chart (-30°)

And with a right ascension angle of 60° we obtain:

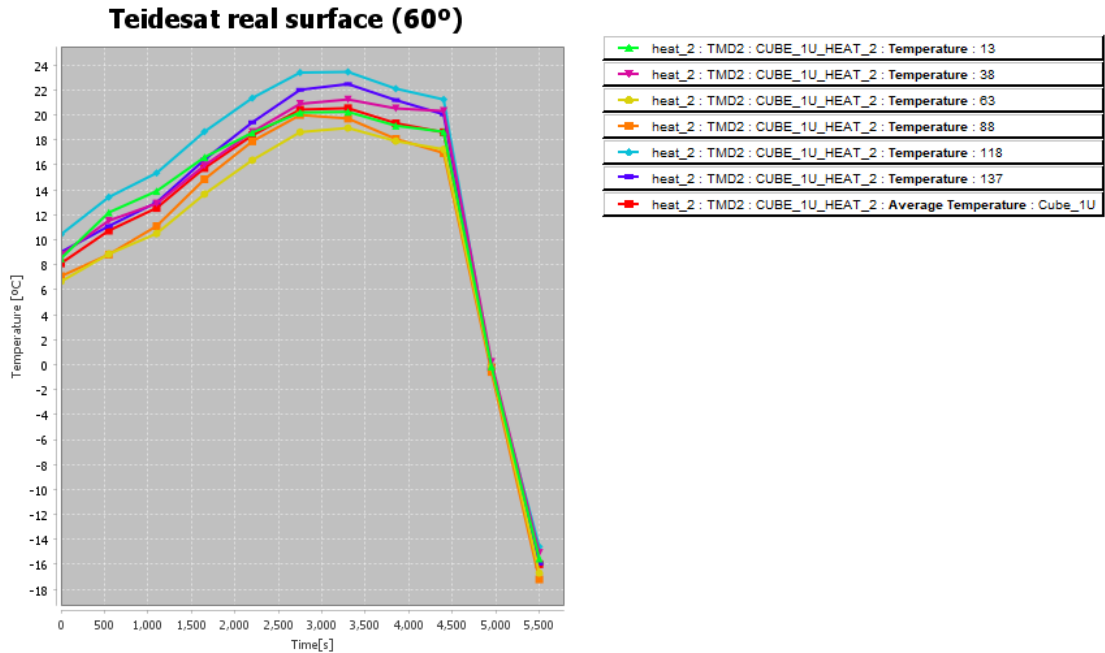


Figure 16: Teidesat temperature chart (60°)

### ALISIO CASE

As we are not considering thickness in the surfaces, an error is being added in the temperature calculation for this model, so a mesh will be applied and different thickness of the material will be applied in order to check how this affects the results.

Also 2 inner heat sources, one from the instrument and other for the platform (5W and 2W) will be added (unit 1 heats lower face and the upper one 3 of them)

With the surface covered in black anodized, we obtain these temperatures along the surface in one orbit:

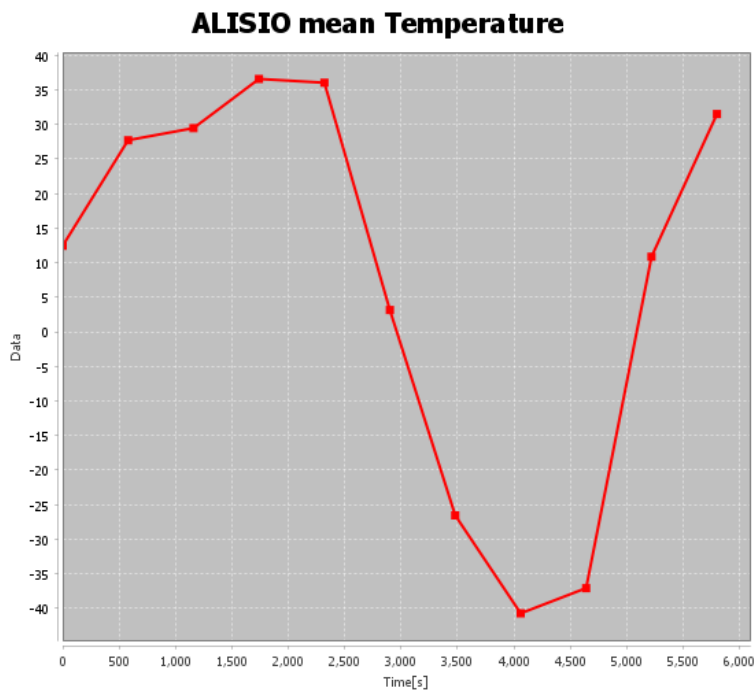


Figure 17: Temperature-time graph in one orbit

Now a temperature from each face will be represented



### ALISIO mean Temperature

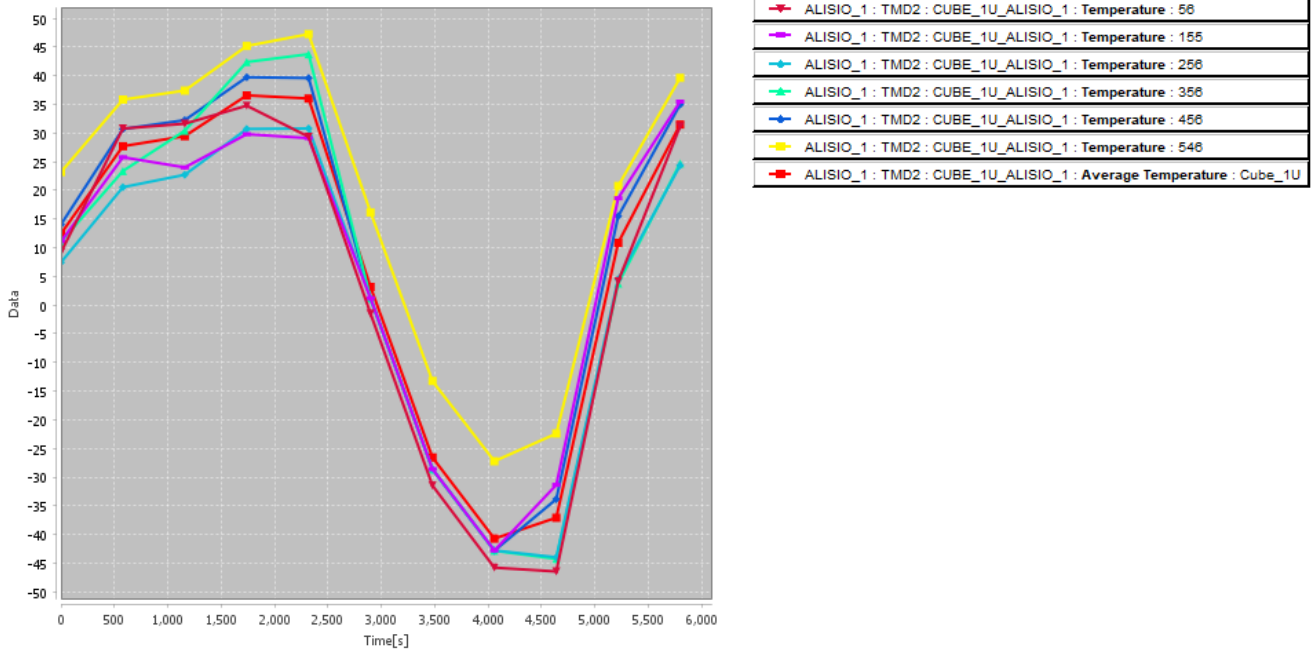


Figure 18: Temperature-time graph in one orbit



If the surface were thicker, the temperature gap would grow smaller.

### ALISIO Anodize Black 2 mm

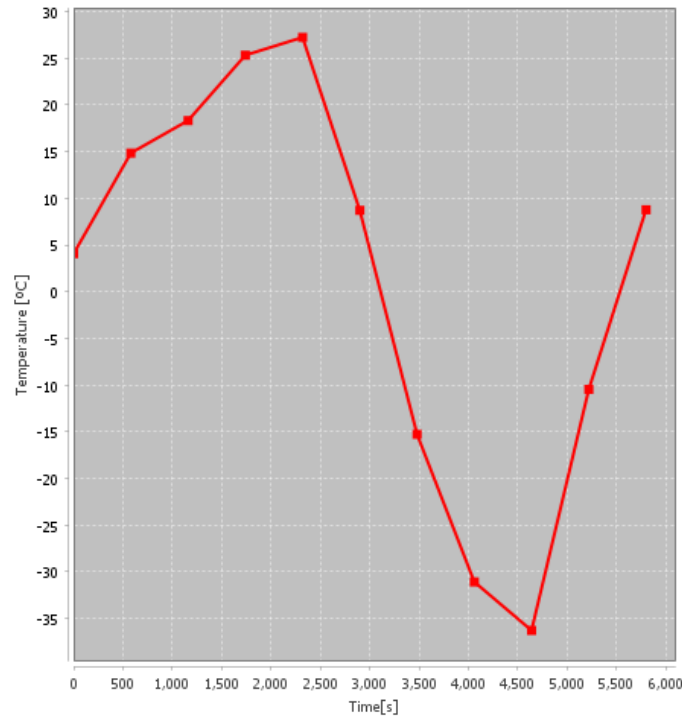


Figure 19: Temperature-time graph in one orbit

### ALISIO Anodize Black 5 mm

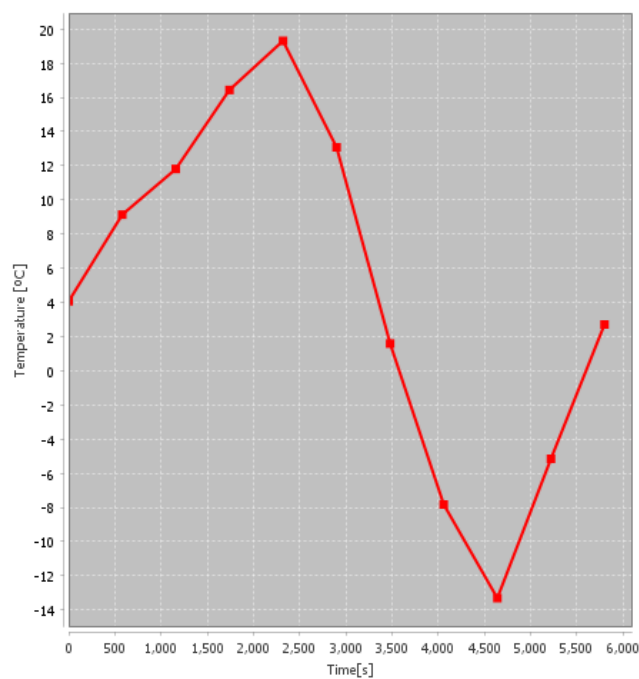





Figure 20: Temperature-time graph in one orbit



Page: 40 of 40	Thermal analysis for the Teidesat / Alisio CubeSat			
----------------	--	--	---	---

It is observed that as the thickness increases the time is needed for the heat sources to heat the spacecraft (there is mass to heat up) and both the maximum and minimum are less significant.

## 6. Conclusions and future work

Studies of how the temperature of the surface of the spacecraft is affected by the space heat sources has been performed resulting in some useful data of how to proceed in future phases (thermal design).

Both satellites analysed happen to be in LEO and neither of them have a significant size, so an optical set of high absorptivity and a little smaller emissivity (around 0,8) should give good surface temperatures. This temperature is the one of the outer surface, some of the heat absorbed by the surface will be radiated or conducted to the inner parts (the ones sensible to temperatures), but that will be deeply analysed in the future, as none of the satellites have the inner disposition fully designed.

In San Cristóbal de La Laguna, on 14<sup>th</sup> of June 2019

Javier González Vilar

Fdo:





**Final Bachelor Thesis**

---

# THERMAL ANALYSIS FOR THE TEIDESAT / ALISIO CUBESATS

---

## **ANNEX 1 Calculations**

**Studies:**

Mechanical Engineering Bachelor

**Author:**

Javier González Vilar

**JUNE 2019**



*Page intentionally left in blank*

## Annex 1

1. Calculation from 4.5. developed .....	3
2. Times of eclipse .....	6



## 1. Calculation from 4.5. developed

If we choose anodize black for the rest of the surface temperature goes as (from 4.5.):

Value of the solar cells			Value of the material (anodize black)		Combination values		Final temperature	
$\alpha_\lambda$	$\epsilon_{IR}$	name of cells	$\alpha_\lambda$	$\epsilon_{IR}$	total $\alpha$	total $\epsilon$	T(K)	T(°C)
0,78	0,82	AE	0,88	0,88	0,82	0,844	328,144951	54,9949509
0,82	0,85	AMSAT	0,88	0,88	0,844	0,862	328,652697	55,5026965
0,77	0,8	ATN Black	0,88	0,88	0,814	0,832	328,75096	55,6009605
0,86	0,85	ATN blue	0,88	0,88	0,868	0,862	330,842411	57,6924115
0,91	0,81	GOES	0,88	0,88	0,898	0,838	335,882568	62,7325676
0,77	0,81	IUE	0,88	0,88	0,814	0,838	328,160917	55,0109175
0,79	0,82	SSS	0,88	0,88	0,826	0,844	328,710827	55,5608273

Table 12: Anodize black combinations

This temperature seems to high, so we try with another material with less absorptivity or higher emissivity (or both), like gold.

Value of the solar cells			Value of the material (gold)		Combination values		Final temperature	
$\alpha_\lambda$	$\epsilon_{IR}$	name of cells	$\alpha_\lambda$	$\epsilon_{IR}$	total $\alpha$	total $\epsilon$	T(K)	T(°C)
0,78	0,82	AE	0,48	0,82	0,66	0,82	314,097537	40,9475368
0,82	0,85	AMSAT	0,48	0,82	0,684	0,838	315,013039	41,8630394
0,77	0,8	ATN Black	0,48	0,82	0,654	0,808	314,586856	41,4368562
0,86	0,85	ATN blue	0,48	0,82	0,708	0,838	317,565389	44,4153889
0,91	0,81	GOES	0,48	0,82	0,738	0,814	323,009673	49,8596731
0,77	0,81	IUE	0,48	0,82	0,654	0,814	314,005541	40,8555414
0,79	0,82	SSS	0,48	0,82	0,666	0,82	314,761281	41,6112808

Table 13: Gold combinations

Now the maximum T enters inside our requisites, but it is too close to the limit.



Alzac A-2 Surface do give good results

Value of the solar cells			Value of the material (Alzac A-2)		Combination values		Final temperature	
$\alpha_\lambda$	$\epsilon_{IR}$	name of cells	$\alpha_\lambda$	$\epsilon_{IR}$	total $\alpha$	total $\epsilon$	T(K)	T(°C)
0,78	0,82	AE	0,16	0,73	0,532	0,784	302,185499	29,035499
0,82	0,85	AMSAT	0,16	0,73	0,556	0,802	303,538907	30,3889072
0,77	0,8	ATN Black	0,16	0,73	0,526	0,772	302,56485	29,4148502
0,86	0,85	ATN blue	0,16	0,73	0,58	0,802	306,51229	33,3622901
0,91	0,81	GOES	0,16	0,73	0,61	0,778	312,475822	39,3258217
0,77	0,81	IUE	0,16	0,73	0,526	0,778	301,979804	28,8298042
0,79	0,82	SSS	0,16	0,73	0,538	0,784	302,964554	29,8145545

Table 14: Alzac A-2 combinations

As well as the composite coating GSFC SiOx Al<sub>2</sub>O<sub>3</sub>-Ag

Value of the solar cells			Value of the material (GSFC SiOx Al <sub>2</sub> O <sub>3</sub> -Ag)		Combination values		Final temperature	
$\alpha_\lambda$	$\epsilon_{IR}$	name of cells	$\alpha_\lambda$	$\epsilon_{IR}$	total $\alpha$	total $\epsilon$	T(K)	T(°C)
0,78	0,82	AE	0,07	0,68	0,496	0,764	299,307006	26,1570057
0,82	0,85	AMSAT	0,07	0,68	0,52	0,782	300,80108	27,6510805
0,77	0,8	ATN Black	0,07	0,68	0,49	0,752	299,661316	26,5113157
0,86	0,85	ATN blue	0,07	0,68	0,544	0,782	303,931666	30,7816657
0,91	0,81	GOES	0,07	0,68	0,574	0,758	310,121001	36,9710008
0,77	0,81	IUE	0,07	0,68	0,49	0,758	299,06655	25,91655
0,79	0,82	SSS	0,07	0,68	0,502	0,764	300,129533	26,9795334

Table 15: GSFC SiOx Al<sub>2</sub>O<sub>3</sub>-Ag combinations



And 2 mil of Aclar film (aluminium backing)

Value of the solar cells			Value of the material (2mil Aclar film )		Combination values		Final temperature	
$\alpha_\lambda$	$\epsilon_{IR}$	name of cells	$\alpha_\lambda$	$\epsilon_{IR}$	total $\alpha$	total $\epsilon$	T(K)	T(°C)
0,78	0,82	AE	0,11	0,62	0,512	0,74	303,900868	30,7508676
0,82	0,85	AMSAT	0,11	0,62	0,536	0,758	305,268561	32,1185611
0,77	0,8	ATN Black	0,11	0,62	0,506	0,728	304,324269	31,1742695
0,86	0,85	ATN blue	0,11	0,62	0,56	0,758	308,359837	35,2098373
0,91	0,81	GOES	0,11	0,62	0,59	0,734	314,618208	41,468208
0,77	0,81	IUE	0,11	0,62	0,506	0,734	303,700438	30,5504378
0,79	0,82	SSS	0,11	0,62	0,518	0,74	304,712236	31,5622358

Table 16: Aclar film combinations

### Cold Case

solar cells values (fixed) ATN black		Surface values			Combined values		Final temperature	
$\alpha_\lambda$	$\epsilon_{IR}$	Surface	$\alpha_\lambda$	$\epsilon_{IR}$	total $\alpha$	total $\epsilon$	T(K)	T (°C)
0,77	0,8	Al 6061 T6	0,031	0,039	0,4744	0,4956	181,408984	-91,7410158
0,77	0,8	Anodize black	0,88	0,88	0,814	0,832	159,371546	-113,778454
0,77	0,8	Velestat black plastic	0,96	0,85	0,846	0,82	159,951439	-113,198561
0,77	0,8	Varium sulphate with white polyvinyl alcohol	0,06	0,88	0,486	0,832	159,371546	-113,778454
0,77	0,8	Hughson white paint Z255	0,25	0,89	0,562	0,836	159,180567	-113,969433
0,77	0,8	Blue anodized titanium foil	0,7	0,13	0,742	0,532	178,222983	-94,9270172
0,77	0,8	Gold	0,48	0,82	0,654	0,808	160,542039	-112,607961
0,77	0,8	Ethanol C black	0,97	0,77	0,85	0,788	161,551153	-111,598847

Table 17: ATN black combinations



## 2. Times of eclipse

For Teidesat

Next, the Earth's angular radius at mission altitude is given by[20]:

$$\rho = \sin^{-1} \left( \frac{R_{Earth}}{R_{Earth} + h_{mission}} \right) = \sin^{-1} \left( \frac{6378}{6378 + 400} \right) = 70,2^{\circ} \text{ (ec. 10)}$$

$$v_{orb} = \sqrt{\frac{GM}{r}} = \sqrt{\frac{6,674 * 10^{-11} \frac{N * m^2}{kg^2} * 5,972 * 10^{24} kg}{(6371 + 400) * 10^3 m}} = 7672,31 \frac{m}{s} \text{ (ec. 11)}$$

$$P = 2\pi * \frac{6371 + h}{v_{orb}} = 2\pi * \frac{(6371 + 400) * 10^3}{7672,31} = 5545,06 \text{ sec (ec. 12)}$$

The maximum time of eclipse (TE) and the time in sunlight (TS) are given by[20]:

$$TE = \frac{2\rho}{360^{\circ}} P = \frac{2 * 70,2^{\circ}}{360^{\circ}} 5545,06 = 2162,5 \text{ seconds} = 36,04 \text{ minutes (ec. 13)}$$

$$TS = P - TE = 5545,06 - 2162,5 = 3382,56 \text{ seconds} = 56,37 \text{ minutes (ec. 14)}$$

For ALISIO:

$$\rho = \sin^{-1} \left( \frac{R_{Earth}}{R_{Earth} + h_{mission}} \right) = \sin^{-1} \left( \frac{6378}{6378 + 600} \right) = 66,0662^{\circ}$$

$$v_{orb} = \sqrt{\frac{GM}{r}} = \sqrt{\frac{6,674 * 10^{-11} \frac{N * m^2}{kg^2} * 5,972 * 10^{24} kg}{(6371 + 600) * 10^3 m}} = 7561,456 \text{ m/s}$$

$$P = 2\pi * \frac{6371 + h}{v_{orb}} = 2\pi * \frac{(6371 + 600) * 10^3}{7561,456} = 5792,54 \text{ sec}$$

The maximum time of eclipse (TE) and the time in sunlight (TS) are given by[20]:

$$TE = \frac{2\rho}{360^{\circ}} P = \frac{2 * 66,066^{\circ}}{360^{\circ}} 5792,54 = 2126,055 \text{ seconds} = 35,4 \text{ minutes}$$

$$TS = P - TE = 5792,54 - 2126,92 = 3666,48 \text{ seconds} = 61,1 \text{ minutes}$$





It is important to keep in mind that the inclination (Beta) changes drastically the time of eclipse.

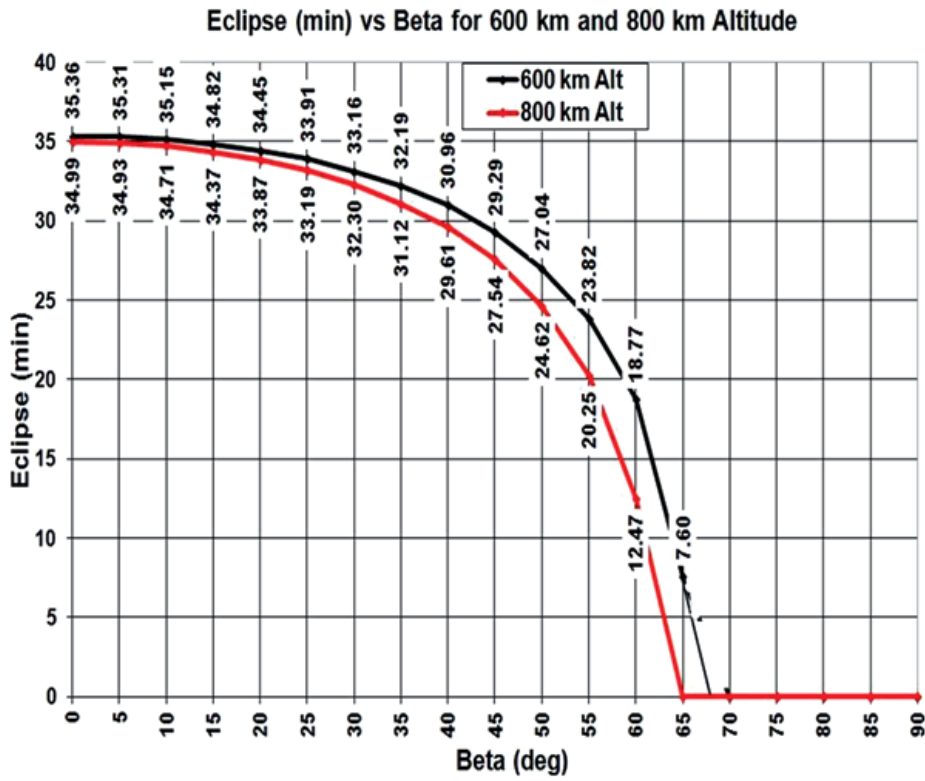


Figure 21: Eclipse time vs Beta degree[12]

**Final Bachelor Thesis**

---

# THERMAL ANALYSIS FOR THE TEIDESAT / ALISIO CUBESATS

---

**ANNEX 2: ESATAN-TMS results**

**Studies:**

Mechanical Engineering Bachelor

**Author:**

Javier González Vilar

**JUNE 2019**



*Page intentionally left in blank*

## Annex 2: ESATAN-TMS results

Teidesat case .....	3
ALISIO CASE .....	13



### 1. Teidesat case

Developing of the first model will be explained systematically, and then different surfaces and geometries will be evaluated

In order to define a case in the software the steps to take are these:

- 1) Define de materials that are going to be used in the spacecraft, and their optical sets (surface radiative properties).

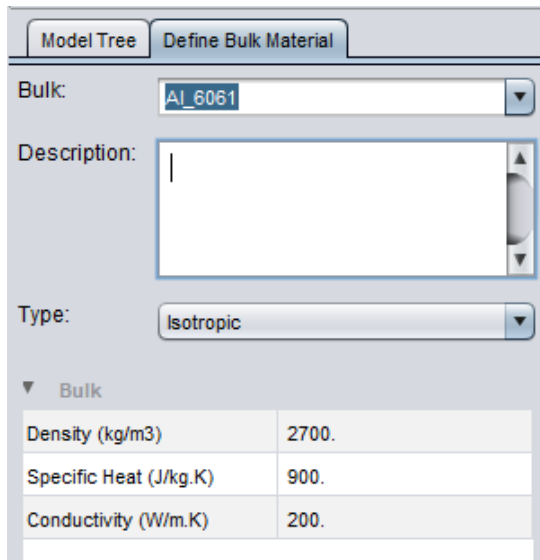


Figure 21: Material definition in ESATAN

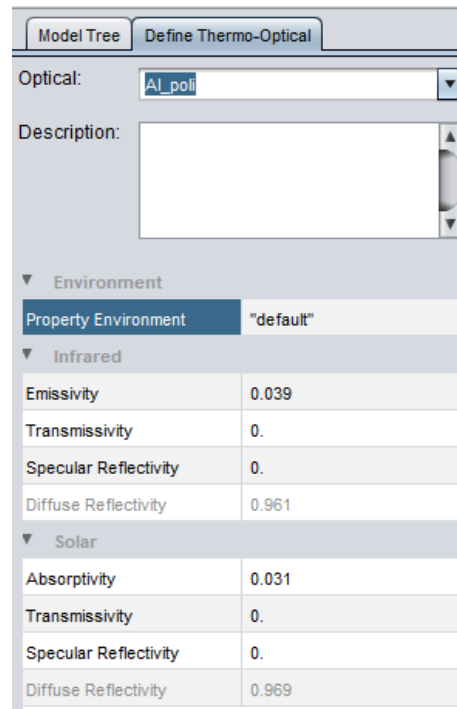


Figure 22: Optical set definition in ESATAN



## 2) Define the geometry of the spacecraft

Params	
height (m)	0.1
xmax (m)	0.1
ymax (m)	0.1
xmin (m)	0.
ymin (m)	0.

Transform	
Method	X Y Z
X Angle (deg)	0.
Y Angle (deg)	0.
Z Angle (deg)	0.
X Distance (m)	0.
Y Distance (m)	0.
Z Distance (m)	0.
Application Order	XR, YR, ZR, XT, YT, ZT

Cutting	
Cutting Sense	"Keep Outside"

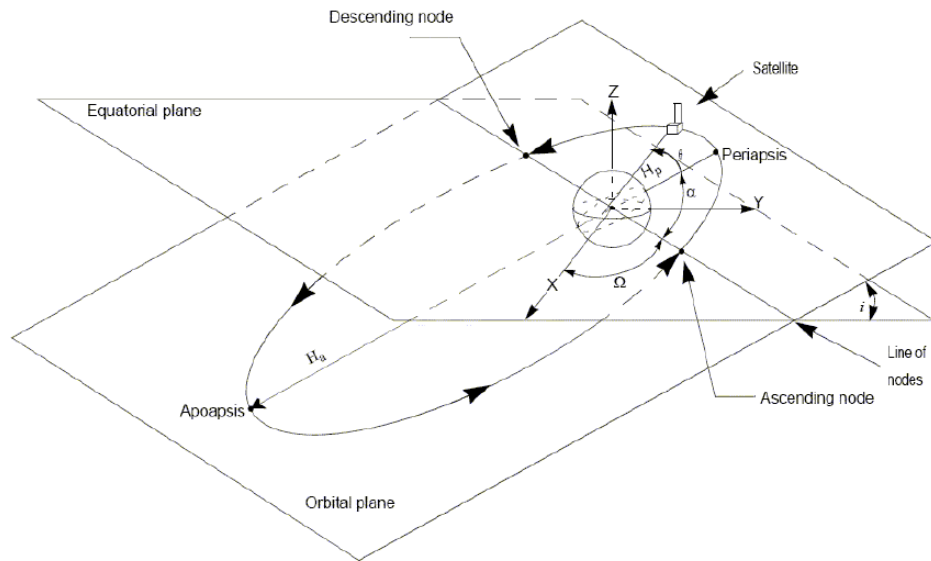
Figure 23: Cube definition in ESATAN

Within the definition non-geometric thermal nodes can be defined, as its name says they are thermal nodes whose physical form is not represented, they are mainly used to define the inner heat generations inside the spacecraft.



Upon ending this definition, the model needs to be assigned and the conductive interfaces between the different parts created need to be defined as well as the user defined conductors (mainly for the non-geometric thermal nodes).

### 3) Define the radiative case



$i$  = inclination  
 $X$  = reference line  
 $\theta$  = true anomaly  
 $\Omega$  = right ascension of the ascending node  
 $\alpha$  = argument of the periapsis  
 $H_a$  = altitude of apogee  
 $H_p$  = altitude of perigee

Figure 24: Orbital parameters

Environment orbit and pointing are to be defined now (environment comes by default, no need to change any data).



Model Tree Radiative Case Dialog

Overview Environment Orbit Pointing

Radiative Case: LEO

Definition Method: Orbit Parameters

Position Method: Angles

▼ Ellipse

Eccentricity	0.0
Semi-Major Axis (m)	6731000.0
Altitude of Apogee (m)	360000.0
Altitude of Perigee (m)	360000.0
Inclination (deg)	51.64
Right Ascension (deg)	0.
Argument of Periapsis (deg)	0.

▼ Arc

Initial True Anomaly (deg)	0.
Final True Anomaly (deg)	360.

▼ Positions

Angle Gap (deg)	45.
Number of Positions	8
True Anomalies Vector (de...)	
Eclipse Entry Exit Points	<input checked="" type="checkbox"/>
Eclipse Offset (deg)	0.5

▼ Ephemeris

Type	Position & Velocity
Longitude (deg)	0.0
Latitude (deg)	0.0
Azimuth (deg)	90.0
Matrix	Not Defined

Figure 25: Orbit definition ESATAN

Model Tree Radiative Case Dialog

Overview Environment Orbit Pointing

Radiative Case: LEO

Celestial Body: Earth

Start Date:

ICS inertial wrt:  Sun  Vernal point

▼ Sun/Planet System

Orbit Centre	PLANET
Planet Radius (m)	6371000.
Gravitational Acceleration ...	9.798
Sun Planet Distance (m)	151149077350.
Solar Declination (deg)	18.287
Sun's Right Ascension (deg)	49.625
Orbital Precession (deg/s)	0.
Sun Radius (m)	695800000.
Celestial Body Image	Earth

▼ Sun Specific

Sun Temperature (K)	5778.
Solar Constant Override (...)	0.
Sun Rays	Parallel Rays
Sun Distance Override (m)	0.

▼ Planet Albedo

Method	UNIFORM
Albedo	0.306

▼ Planet Temperature

Method	UNIFORM
Temperature (K)	254.3
Infra-Red Emissivity	1.

Figure 26: Environment definition ESATAN



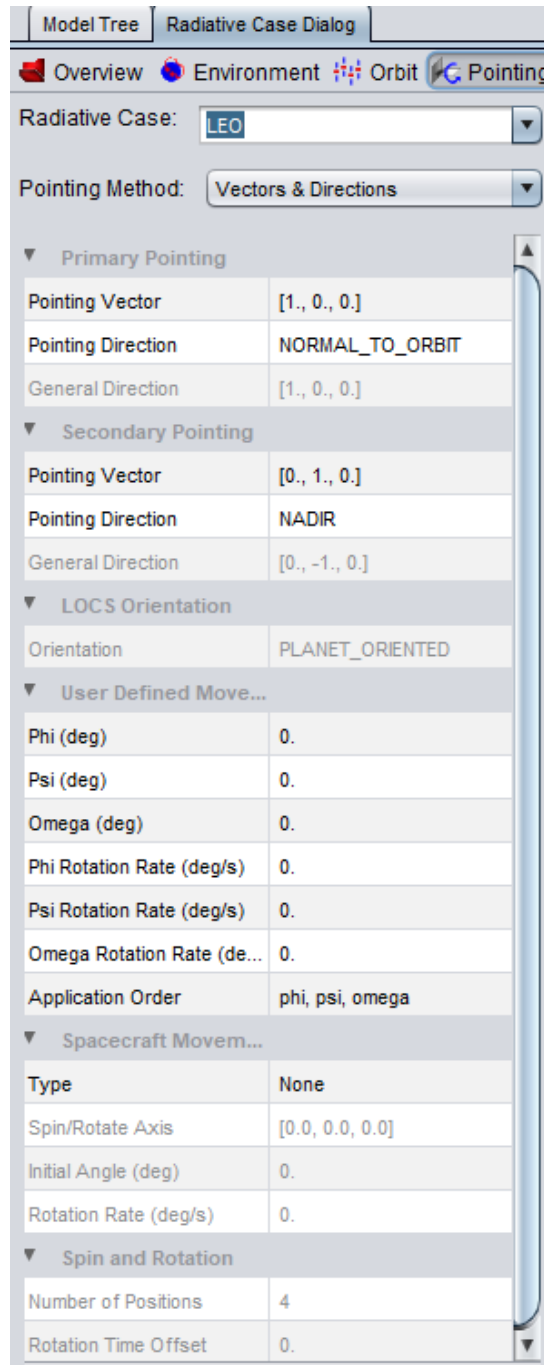


Figure 25: Pointing definition ESATAN



Then this case need to be executed for the program to make the calculation, this is the output:

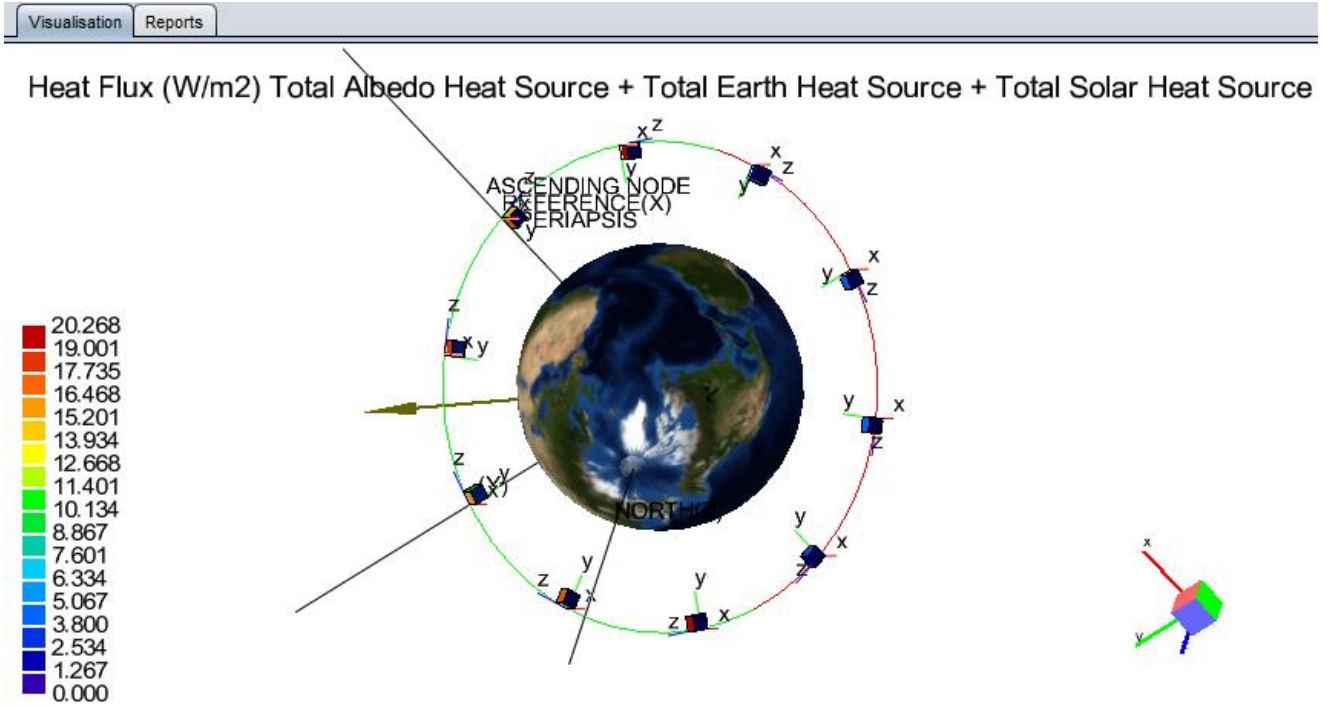


Figure 26: Heat flux and orbital representation via ESATAN

- 4) Define thermal case: before this step we need to define de boundary conditions if any are to be found.



Then we define the input for the analysis :

The screenshot shows the 'Define Analysis Case' dialog box. The 'Analysis Case' dropdown is set to 'heat\_2'. The 'Solver' dropdown is set to 'ESATAN'. The 'Radiative Data' section is expanded, showing 'Analysis Case Type' as 'Single Radiative Case', 'Radiative Case' as 'LEO', and 'Environment Temperature...' as '-270.'. The 'Conductors' section is expanded, showing 'Generated & User-Defined' checked. The 'Boundary Conditions' section is expanded, showing 'Boundary Conditions' as 'Set'. The 'Control Logic' section is expanded, showing 'Solution Control' and 'Output Calls' as 'Defined'. The 'File Optimisation' section is expanded, showing 'Optimised Thermal Solution' checked, 'REF Minimum Deviation' as '0.005', and 'HF Minimum Deviation' as '0.005'.

Radiative Data	
Analysis Case Type	Single Radiative Case
Radiative Case	LEO
Radiative Cases	
Waveband Array (m)	

Conductors	
Generated & User-Defined	<input checked="" type="checkbox"/>
User-Defined Conductors...	All

Boundary Conditions	
Environment Temperature...	-270.
Boundary Conditions	Set

Control Logic	
Parametric Values	Not Set
Initial Conditions	Not Set
Solution Control	Defined
Output Calls	Defined
Generate Min-Max Data	<input type="checkbox"/>

File Optimisation	
Optimised Thermal Solution	<input checked="" type="checkbox"/>
REF Minimum Deviation	0.005
HF Minimum Deviation	0.005

Figure 27: Input for the thermal analysis ESATAN

After the case has been executed, results are ready to post process.



## 5) Post process of the thermal analysis results

All the data can be extracted via graphs; in this case, temperature along on orbit (mean value) will be obtained and compared with results already obtained previously:

Generating a model cube shaped completely made of Aluminum T6-6061; we obtain these temperatures along the orbit

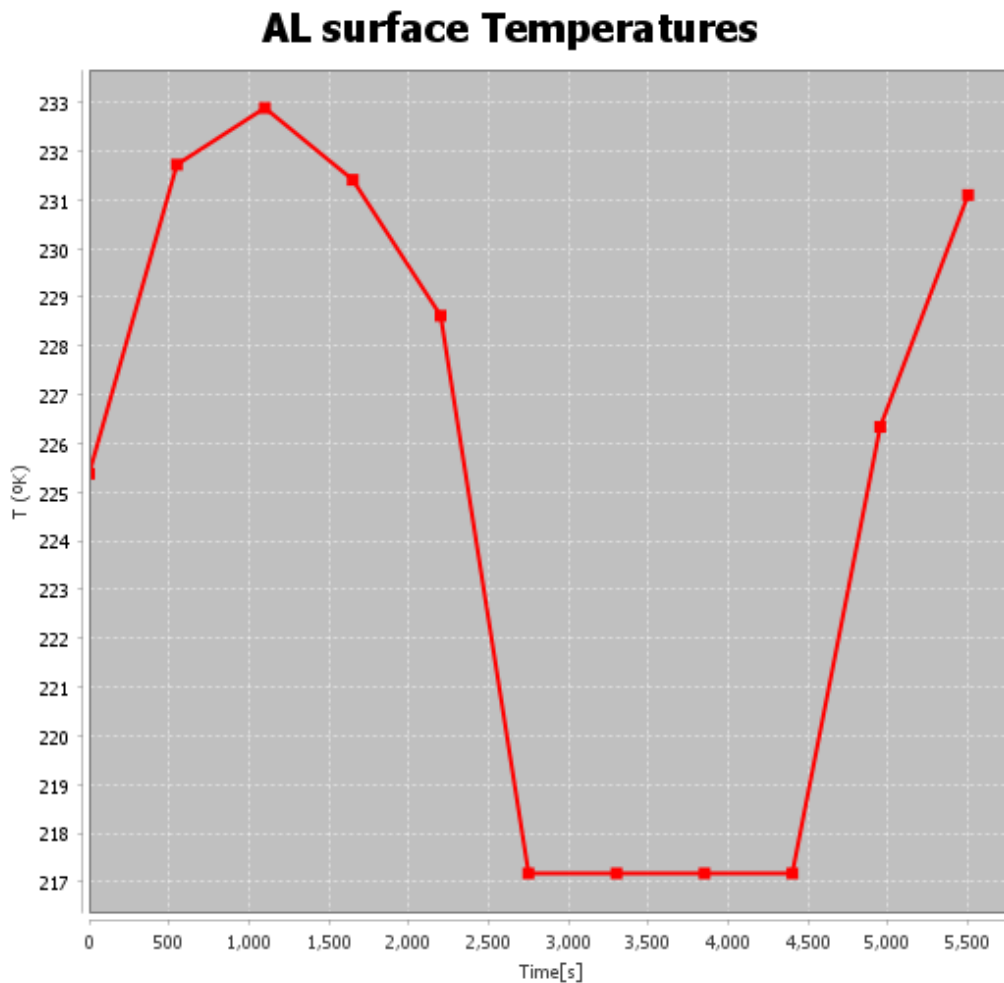


Figure 30: Temperature-time graph in one orbit

Comparing it to the theoretical calculations seen before maximum temperature is quite similar, being the software one 232 °K and the calculated 237 °K (4.3. Cube Case). However this theoretical case is not considering all heat sources, in (4.4) temperature with this surface is 388 °K.

If the surface is anodized aluminium, we have:

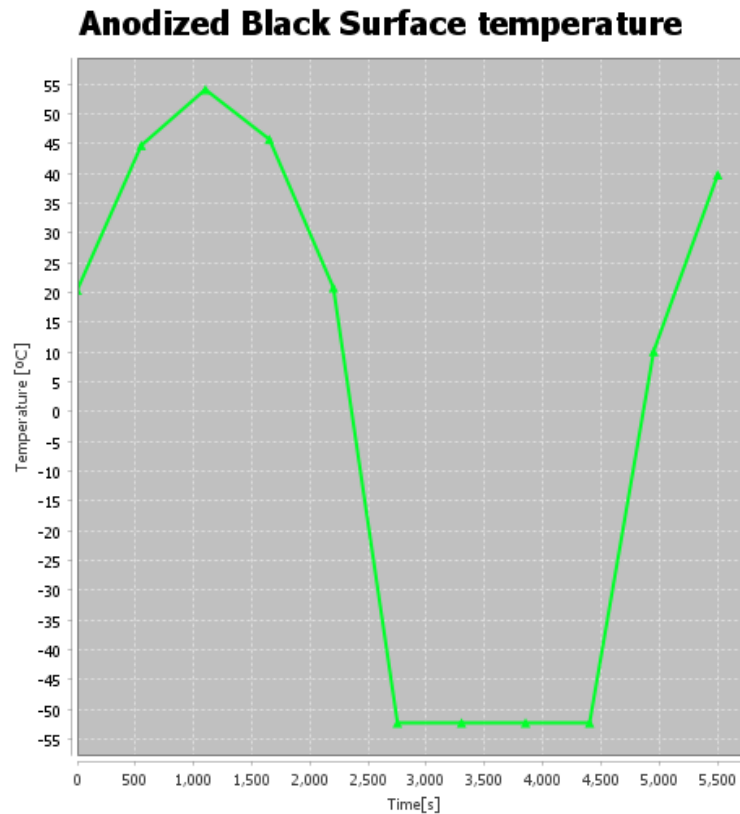


Figure 31: Temperature-time graph in one orbit

Comparing it to the theoretical calculations we observe that maximum temperature is 55°C in the software and 57°C in the calculations performed (4.4. All heat sources case)

For these simulations, the thickness of the satellite walls is being neglected, as well as the inner components and its connections, making them not very precise.

For the purposed material to Teidesat satellite in this document a surface with mesh, real wall thickness and absorptivity and emissivity of the surface will be estimated considering the solar panels

Now surface with mesh, real wall thickness (2mm) and absorptivity and emissivity of the surface will be estimated considering the optical set as the mean value of having solar panels ATN black and anodize black in all surfaces (mean value  $\alpha/\epsilon=0,814/0,832$ ); heat from the payload has been added, but no inner structure is yet considered.

With a right ascension angle of  $-30^\circ$  (high sun exposure along orbit) we obtain:



**Teidesat Real surface (-30°)**

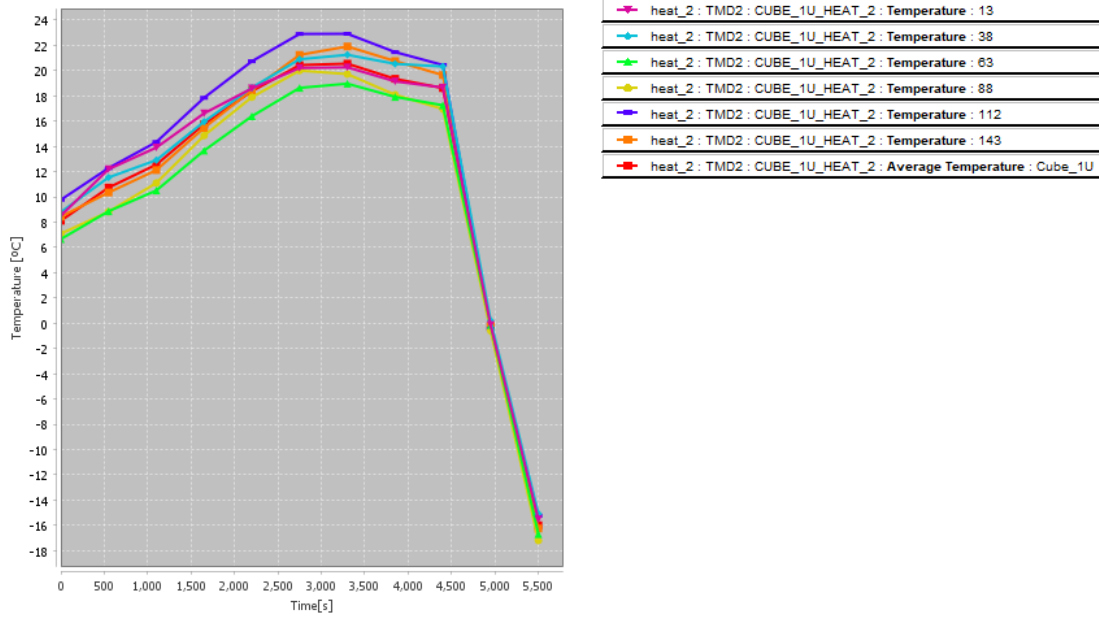


Figure 32: Teidesat temperature chart (-30°)

And with a right ascension angle of 60° we obtain:

**Teidesat real surface (60°)**

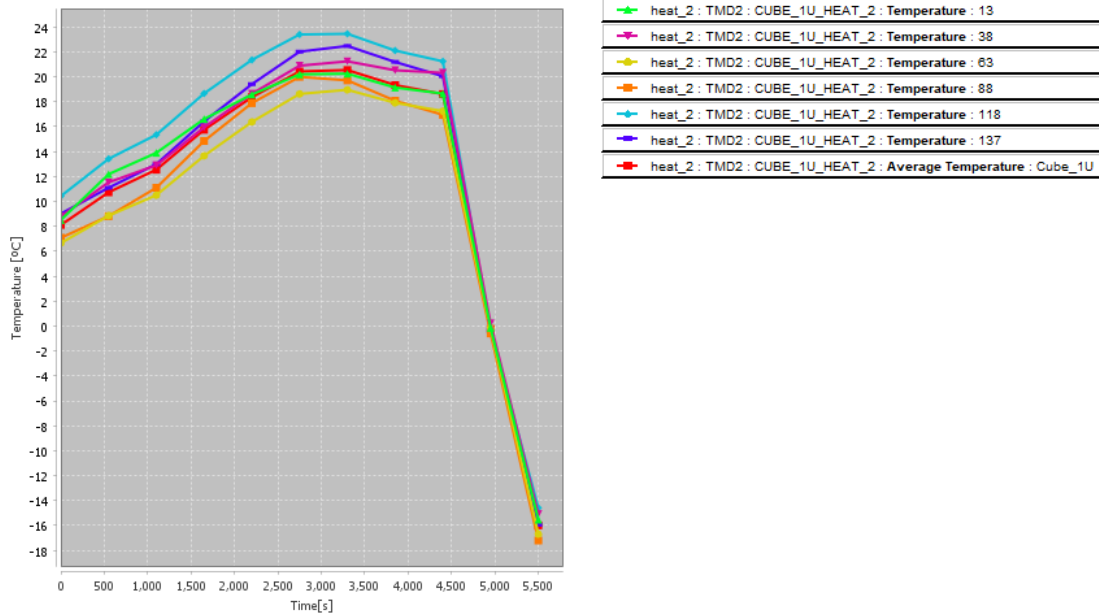


Figure 33: Teidesat temperature chart (60°)



## 2. Alisio case

As we are not considering thickness in the surfaces, an error is being added in the temperature calculation for this model, so a mesh will be applied and different thickness of the material will be applied in order to check how this affects the results.

Also 2 inner heat sources, one from the instrument and other for the platform (5W and 2W) will be added (unit 1 heats lower face and the upper one 3 of them)

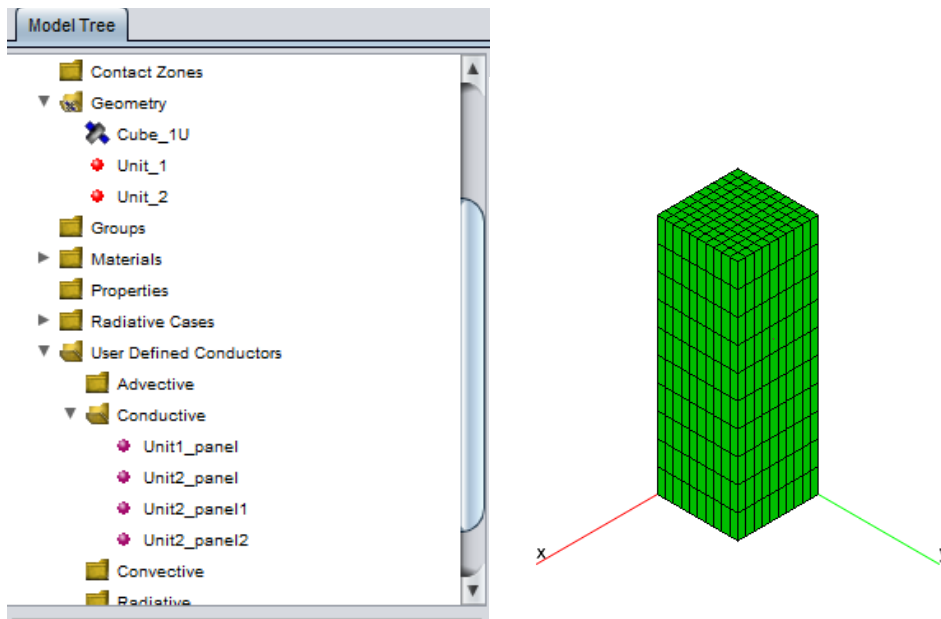


Figure 34: ALISIO geometry



With the surface covered in black anodized, we obtain these temperatures along the surface in one orbit:

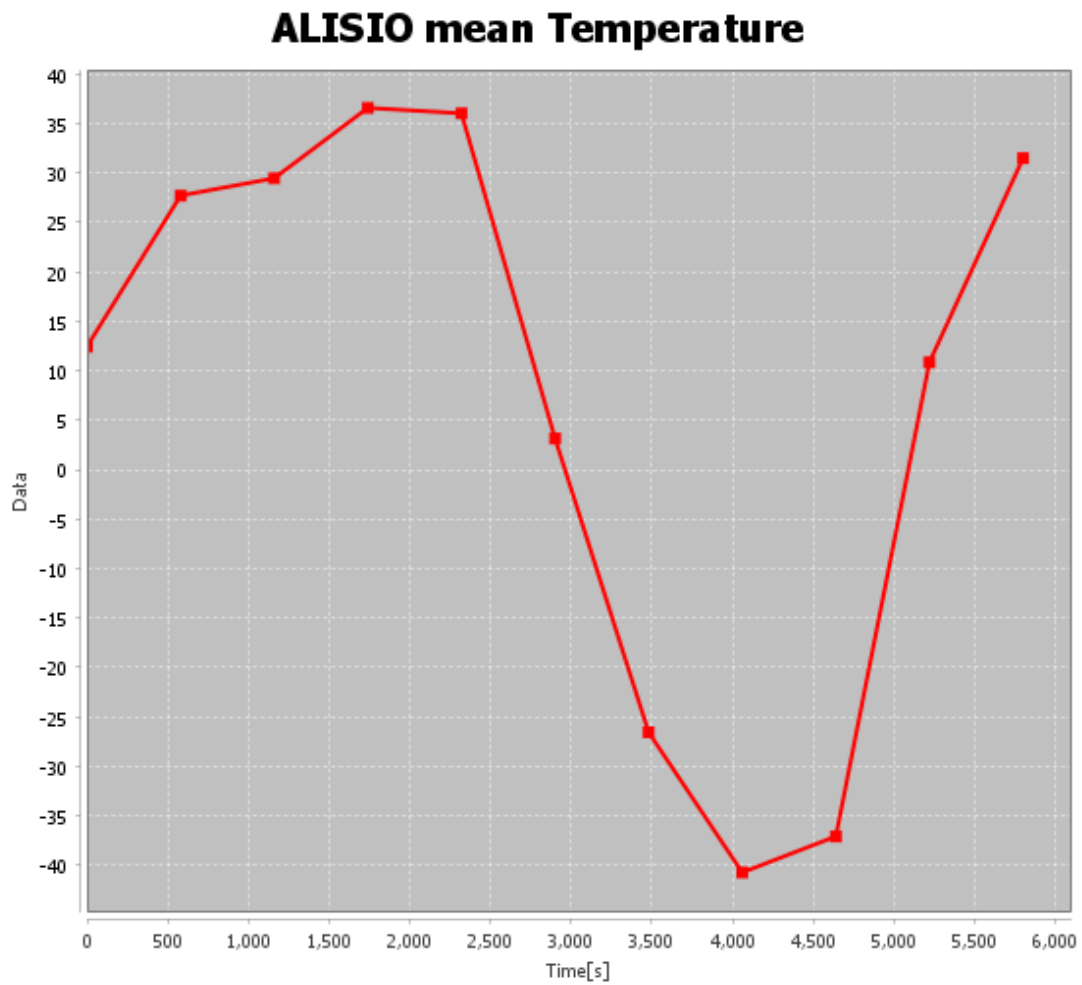


Figure 35: Temperature-time graph in one orbit

Now a node's temperature from each face will be represented





### ALISIO mean Temperature

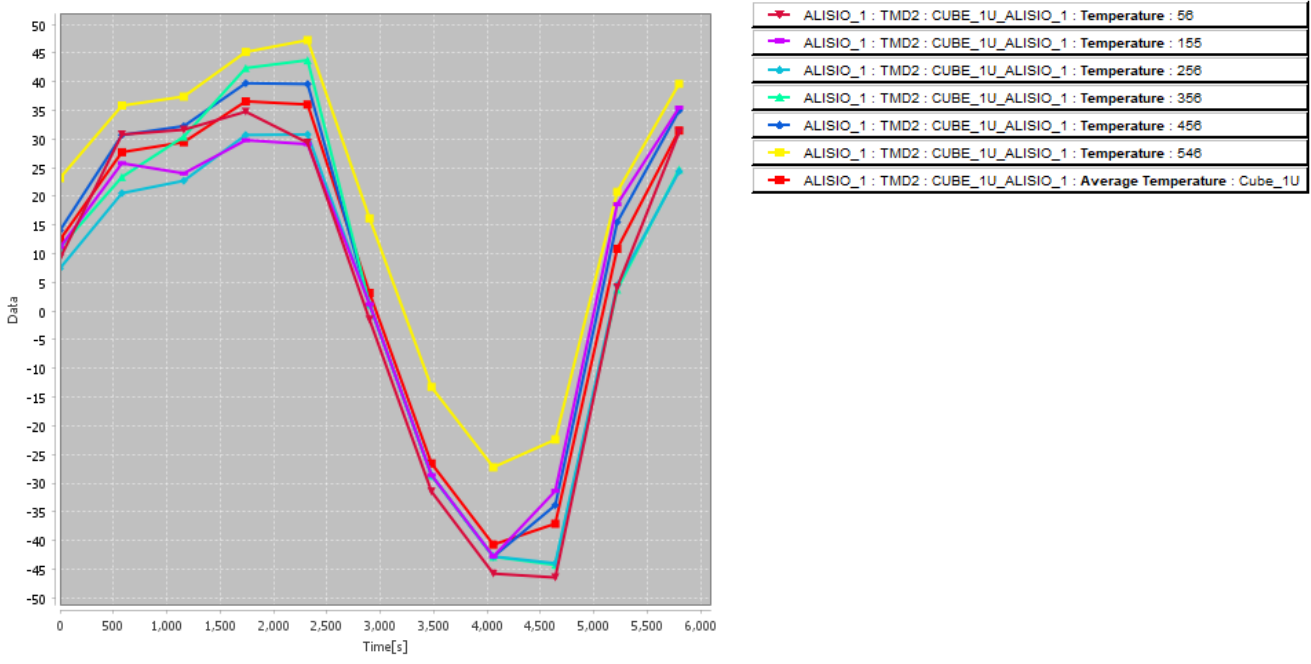


Figure 36: Temperature-time graph in one orbit



If the surface were thicker, the temperature gap would grow smaller.

### ALISIO Anodize Black 2 mm

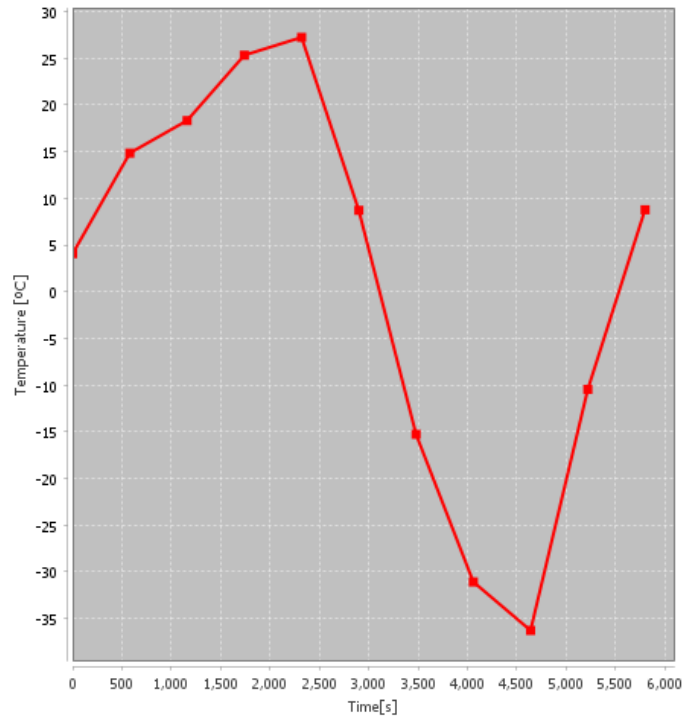


Figure 37: Temperature-time graph in one orbit

### ALISIO Anodize Black 5 mm

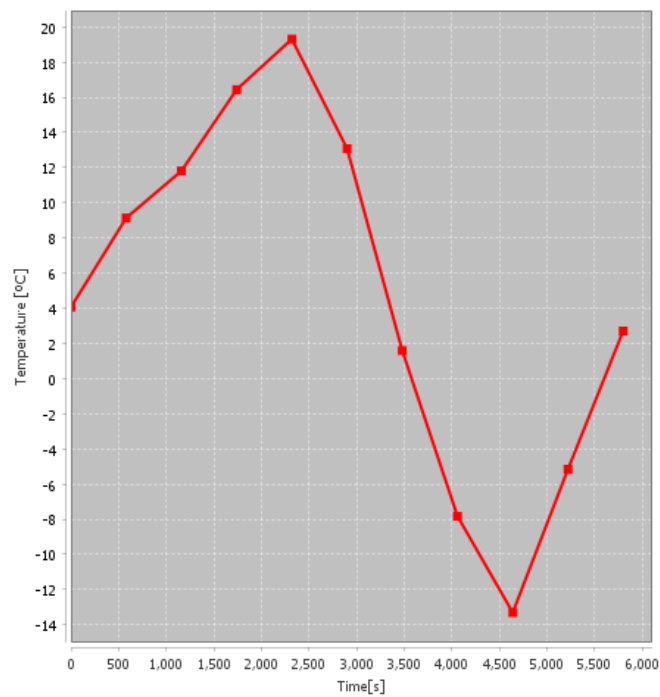


Figure 38: Temperature-time graph in one orbit



It is observed that as the thickness increases more time is needed for the heat sources to heat the spacecraft (there is mass to heat up) and both the maximum and minimum are less significant.



**Final Bachelor Thesis**

---

# THERMAL ANALYSIS FOR THE TEIDESAT / ALISIO CUBESATS

---

**ANNEX 3: Theoretical context**

**Studies:**

Mechanical Engineering Bachelor

**Author:**

Javier González Vilar

**JUNE 2019**



*Page intentionally left in blank*

## Annex 3: Theoretical context

1.	Basics of Heat Transfer .....	3
2.	Conduction.....	3
3.	Convection .....	5
4.	Radiation.....	6
4.1.	The view factor .....	9
4.2.	Heat transfer to or from a surface.....	11
4.3.	Heat transfer between two surfaces .....	12
5.	Orbits.....	13
6.	Environments of Earth orbits.....	23
6.1.	Direct solar .....	24
6.2.	Albedo.....	26
6.3.	Earth IR.....	26
6.4.	Molecular free heating.....	27
6.5.	Charged-particle heating.....	28



## 1. Basics of Heat Transfer

The science of thermodynamics deals with the amount of heat transfer as a system undergoes a process from one equilibrium state to another, and does not refer to how long the process will take. But in engineering, we are often interested in the rate of heat transfer, which is the topic of the science of heat transfer. The three main forms of heat (the form of energy that can be transferred from one system to another as a result of temperature difference) transfer shall be presented: conduction, convection and radiation.

Before that, it is important to have in mind the first law of thermodynamics which states energy can neither be created nor destroyed; it can only change forms. Therefore, every bit of energy must be accounted for during a process. The conservation of energy principle (or the energy balance) for any system undergoing any process may be expressed as follows: The net change (increase or decrease) in the total energy of the system during a process is equal to the difference between the total energy entering and the total energy leaving the system during that process (first thermodynamics law). [21]

$$\left( \begin{array}{c} \text{Total energy entering} \\ \text{the system} \end{array} \right) - \left( \begin{array}{c} \text{Total energy leaving} \\ \text{the system} \end{array} \right) \\ = \text{(Change of the total energy in the system)}$$

In terms of heat we have:

$$Q_{in} - Q_{out} = \Delta Q_{total} \text{ (ec. 15)}$$

## 2. Conduction

Conduction is the transfer of energy from the more energetic particles of a substance to the adjacent less energetic ones as a result of interactions between the particles. Conduction can take place in solids, liquids, or gases. In gases and liquids, conduction is due to the collisions and diffusion of the molecules during their random motion. In solids, it is due to the combination of vibrations of the molecules in a lattice and the energy transport by free electrons. A cold canned drink in a warm room, for example, eventually warms up to the room temperature as a result of heat transfer from the room to the drink through the aluminium can by conduction. The rate of



heat conduction through a medium depends on the geometry of the medium, its thickness, and the material of the medium, as well as the temperature difference across the medium. We know that wrapping a hot water tank with glass wool (an insulating material) reduces the rate of heat loss from the tank. The thicker the insulation, the smaller the heat loss. We also know that a hot water tank will lose heat at a higher rate when the temperature of the room housing the tank is lowered. Further, the larger the tank, the larger the surface area and thus the rate of heat loss. Consider steady heat conduction through a large plane wall of thickness  $x$  and area  $A$ , as shown in Figure 39. The temperature difference across the wall is  $T_2 - T_1$ . Experiments have shown that the rate of heat transfer  $\dot{Q}$  through the wall is doubled when the temperature difference  $T$  across the wall or the area  $A$  normal to the direction of heat transfer is doubled, but is halved when the wall thickness  $L$  is doubled. Thus we conclude that the rate of heat conduction through a plane layer is proportional to the temperature difference across the layer and the heat transfer area, but is inversely proportional to the thickness of the layer (Fourier's law). [21]

$$\dot{Q}_{cond} = kA \frac{\Delta T}{\Delta x} [W] \text{ (ec. 16)}$$

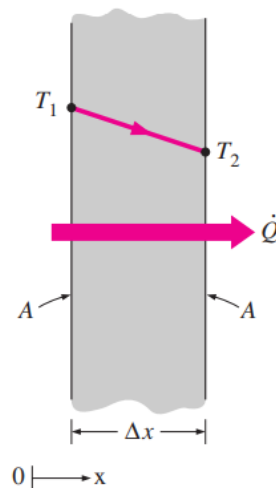


Figure 39: Heat conduction through a large plane Wall [21]

Where

$k$ : thermal conductivity of the material (measure of the ability of a material to conduct heat)

$A$ : Area of the surface





$\Delta T$ : Difference of temperature measured

$\Delta x$ : Distance between points measured (heat direction)

Analogously:

$$\dot{Q}_{cond} = \frac{T_1 - T_2}{R} \quad [W] \quad (ec. 17)$$

Where:

$$R = \frac{L}{kA} = \text{conduction resistance } [^{\circ}\text{C}/\text{W}]$$

$T_1, T_2$ : temperatures of the point within calculation want to be done

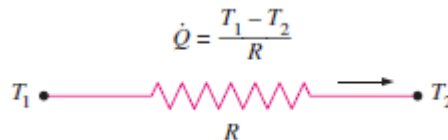


Figure 40: Thermal resistance [21]

### 3. Convection

Convection is the mode of energy transfer between a solid surface and the adjacent liquid or gas that is in motion, and it involves the combined effects of conduction and fluid motion. The faster the fluid motion, the greater the convection heat transfer. In the absence of any bulk fluid motion, heat transfer between a solid surface and the adjacent fluid is by pure conduction. The presence of bulk motion of the fluid enhances the heat transfer between the solid surface and the fluid, but it also complicates the determination of heat transfer rates.

Despite the complexity of convection, the rate of convection heat transfer is observed to be proportional to the temperature difference, and is conveniently expressed by Newton's law of cooling as:

$$\dot{Q}_{conv} = hA_s(T_s - T_{\infty}) \quad [W] \quad (ec. 18)$$



where  $h$  is the convection heat transfer coefficient in  $W/m^2 \cdot ^\circ C$ ,  $A_s$  is the surface area through which convection heat transfer takes place,  $T_s$  is the surface temperature, and  $T_\infty$  is the temperature of the fluid sufficiently far from the surface.

Although this is an important form of heat transfer in earth, in space, where there is not surrounding air, it is not. Therefore, convection in these analyses will be negligible [21].

#### 4. Radiation

Radiation is the energy emitted by matter in the form of electromagnetic waves (or photons) as a result of the changes in the electronic configurations of the atoms or molecules. Unlike conduction and convection, the transfer of energy by radiation does not require the presence of an intervening medium.

In fact, energy transfer by radiation is fastest (at the speed of light) and it suffers no attenuation in a vacuum. This is how the energy of the sun reaches the earth. In heat transfer studies we are interested in thermal radiation, which is the form of radiation emitted by bodies because of their temperature. It differs from other forms of electromagnetic radiation such as x-rays, gamma rays, microwaves, radio waves, and television waves that are not related to temperature. All bodies at a temperature above absolute zero emit thermal radiation.

Radiation is a volumetric phenomenon, and all solids, liquids, and gases emit, absorb, or transmit radiation to varying degrees. However, radiation is usually considered to be a surface phenomenon for solids that are opaque to thermal radiation such as metals, wood, and rocks since the radiation emitted by the interior regions of such material can never reach the surface, and the radiation incident on such bodies is usually absorbed within a few microns from the surface.

The maximum rate of radiation that can be emitted from a surface at an absolute temperature  $T_s$  (in K) is given by the Stefan–Boltzmann law as:

$$\dot{Q}_{emit,max} = \sigma A_s T_s^4 \text{ [W]} \text{ (ec. 19)}$$

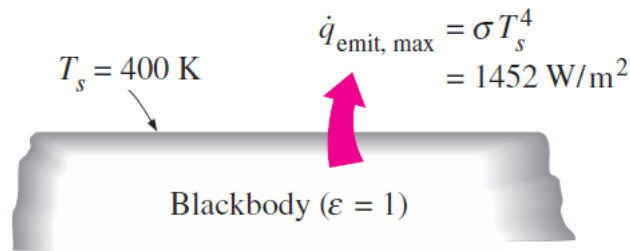


Figure 41: Blackbody radiation [21]

Where  $\sigma=5,67 \cdot 10^{-8} \text{ W/m}^2$  is the Stefan–Boltzmann constant. The idealized surface that emits radiation at this maximum rate is called a blackbody, and the radiation emitted by a blackbody is called blackbody radiation (Fig. 41). The radiation emitted by all real surfaces is less than the radiation emitted by a blackbody at the same temperature, and is expressed as:

$$\dot{Q}_{emit} = \varepsilon \sigma A_s T_s^4 \quad [W] \quad (ec. 20)$$

where  $\varepsilon$  is the emissivity of the surface. The property emissivity, whose value is in the range  $0 \leq \varepsilon \leq 1$ , is a measure of how closely a surface approximates a blackbody for which  $\varepsilon=1$ .

Another important radiation property of a surface is its absorptivity  $\alpha$ , which is the fraction of the radiation energy incident on a surface that is absorbed by the surface. Like emissivity, its value is in the range  $0 \leq \alpha \leq 1$ . A blackbody absorbs the entire radiation incident on it. That is, a blackbody is a perfect absorber ( $\alpha=1$ ) as it is a perfect emitter.

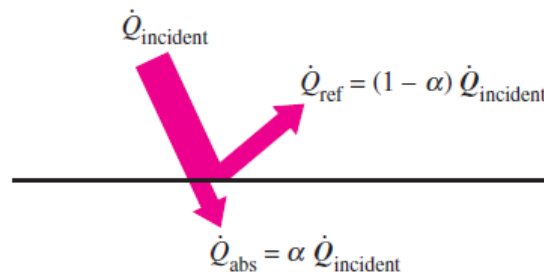


Figure 42: The absorption of radiation incident on



In general, both  $\alpha$  and  $\epsilon$  of a surface depends on the temperature of the surface as well as the wavelength and the direction of the emitted/absorbed radiation. Kirchhoff's law of radiation states that the emissivity and the absorptivity of a surface at a given temperature and wavelength are equal. In many practical applications, the surface temperature and the temperature of the source of incident radiation are of the same order of magnitude, and the average absorptivity of a surface is taken to be equal to its average emissivity

**Real surface:**  
 $\epsilon_\theta \neq \text{constant}$   
 $\epsilon_\lambda \neq \text{constant}$

**Diffuse surface:**  
 $\epsilon_\theta = \text{constant}$

**Gray surface:**  
 $\epsilon_\lambda = \text{constant}$

**Diffuse, gray surface:**  
 $\epsilon = \epsilon_\lambda = \epsilon_\theta = \text{constant}$

In practice, it is usually more convenient to work with radiation properties averaged over all directions, called hemispherical properties. And also, the gray and diffuse approximations are often utilized in radiation calculations. A surface is said to be diffuse if its properties are independent of direction, and gray if its properties are independent of wavelength[21].

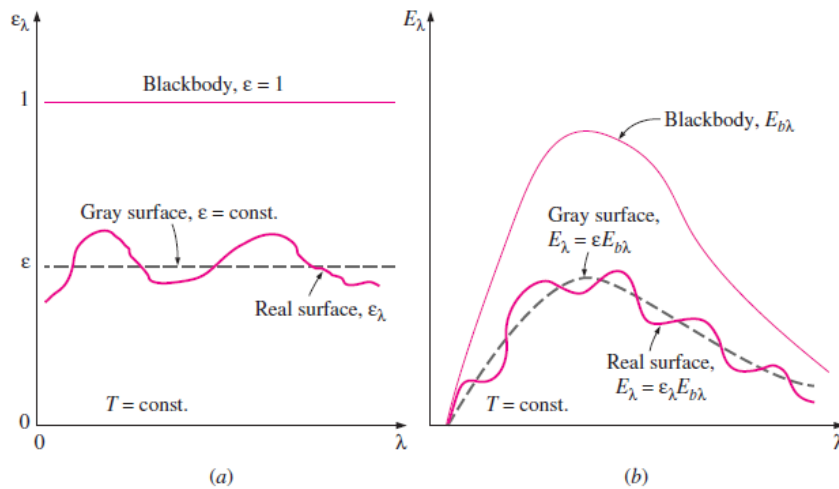


Figure 43: The effect of diffuse and gray approximations on the emissivity of a surface [21]

Figure 44: Comparison of the emissivity of a real surface with those of a gray surface and a blackbody at the same temperature [21]



#### 4.1. The view factor

Radiation heat transfer between surfaces depends on the orientation of the surfaces relative to each other as well as their radiation properties and temperatures. To account for the effects of orientation on radiation heat transfer between two surfaces, we define a new parameter called the view factor, which is a purely geometric quantity and is independent of the surface properties and temperature. It is also called the shape factor, configuration factor, and angle factor. The view factor based on the assumption that the surfaces are diffuse emitters and diffuse reflectors is called the diffuse view factor, and the view factor based on the assumption that the surfaces are diffuse emitters but specular reflectors is called the specular view factor. It will be considered radiation exchange between diffuse surfaces only, and thus the term view factor will simply mean diffuse view factor.

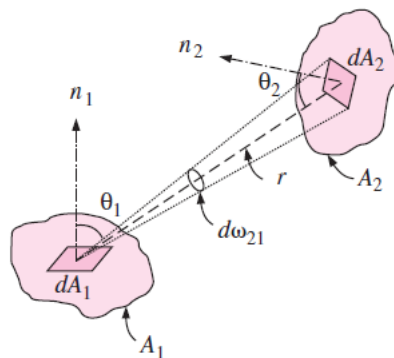


Figure 45: The view factor [21]

The view factor from a surface  $i$  to a surface  $j$  is denoted by  $F_{i \rightarrow j}$  or just  $F_{ij}$ , and is defined as:

$F_{ij}$  = the fraction of the radiation leaving surface  $i$  that strikes surface  $j$  directly

To develop a general expression for the view factor, consider two differential surfaces  $dA_1$  and  $dA_2$  on two arbitrarily oriented surfaces  $A_1$  and  $A_2$ , respectively, as shown in Fig.45 with the parameters as shown in the figure we end up having:

$$dF_{dA_1 \rightarrow dA_2} = \frac{\dot{Q}_{dA_1 \rightarrow dA_2}}{\dot{Q}_{dA_1}} = \frac{\cos\theta_1 \cos\theta_2}{\pi r^2} dA_2 \quad (ec. 21)$$

$$F_{dA_1 \rightarrow A_2} = \int_{A_2} \frac{\cos\theta_1 \cos\theta_2}{\pi r^2} dA_2$$



$$F_{12} = F_{A_1 \rightarrow A_2} = \frac{\dot{Q}_{A_1 \rightarrow A_2}}{\dot{Q}_{A_1}} = \frac{1}{A_1} \int_{A_1} \int_{A_2} \frac{\cos\theta_1 \cos\theta_2}{\pi r^2} dA_1 dA_2$$

Noting that:

$$A_1 F_{12} = A_2 F_{21}$$

Then we will add this value to the calculation of the heat transfer that we already know. For a black surface this will be:

$$\dot{Q}_{1 \rightarrow 2} = A_1 F_{1 \rightarrow 2} \sigma (T_1^4 - T_2^4) [W] \text{ (ec. 22)}$$

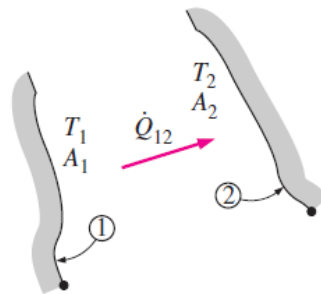


Figure 46: Heat transfer between 2 surfaces [21]

The analysis of radiation transfer in enclosures consisting of black surfaces is relatively easy, but most enclosures encountered in practice involve nonblack surfaces, which allow multiple reflections to occur. Radiation analysis of such enclosures becomes very complicated unless some simplifying assumptions are made.

To make a simple radiation analysis possible, it is common to assume the surfaces of an enclosure to be opaque, diffuse, and gray. That is, the surfaces are non-transparent, they are diffuse emitters and diffuse reflectors, and their radiation properties are independent of wavelength. Also, each surface of the enclosure is isothermal, and both the incoming and outgoing radiation are uniform over each surface[21].



#### 4.2. Heat transfer to or from a surface

During a radiation interaction, a surface loses energy by emitting radiation and gains energy by absorbing radiation emitted by other surfaces. A surface experiences a net gain or a net loss of energy, depending on which quantity is larger. The net rate of radiation heat transfer from a surface  $i$  of surface area  $A_i$  is denoted by  $\dot{Q}_i$  and is expressed as:

$$\dot{Q}_i = \left( \text{Radiation leaving entire surface } i \right) - \left( \text{Radiation incident on entire surface } i \right) = A_i(J_i - G_i) \text{ [W]}$$

Analogously:

$$\dot{Q}_i = \frac{E_{bi} - J_i}{R_i} \text{ [W]} \text{ (ec. 23)}$$

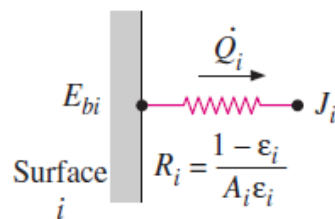


Figure 47: Surface resistance radiation [21]

Where:

$$R_i = \frac{1 - \epsilon_i}{A_i \epsilon_i} \text{ = is the surface resistance radiation}$$

$J_i$ = Radiosity (reflected radiation plus emitted radiation)

$E_{bi}$ = the emissive power of a blackbody at the temperature of the surface (equal to radiosity for black bodies, which means zero resistance for them)

It will be from the surface if  $E_{bi} > J_i$  and to the surface if  $J_i > E_{bi}$  [21].



### 4.3. Heat transfer between two surfaces

Consider two diffuse, gray, and opaque surfaces of arbitrary shape maintained at uniform temperatures, as shown in Figure 48. Recognizing that the radiosity  $J$  represents the rate of radiation leaving a surface per unit surface area and that the view factor  $F_{i \rightarrow j}$  represents the fraction of radiation leaving surface  $i$  that strikes surface  $j$ , the net rate of radiation heat transfer from surface  $i$  to surface  $j$  can be expressed as:

$$\begin{aligned}\dot{Q}_{i \rightarrow j} &= \left( \text{radiation leaving the entire surface } i \text{ that strikes surface } j \right) - \left( \text{radiation leaving the entire surface } j \text{ that strikes surface } i \right) \\ &= A_i J_i F_{i \rightarrow j} - A_j J_j F_{j \rightarrow i} \quad [W]\end{aligned}$$

Applying  $A_i F_{i \rightarrow j} = A_j F_{j \rightarrow i}$  then:

$$\dot{Q}_{i \rightarrow j} = A_i F_{i \rightarrow j} (J_i - J_j) \quad [W] \quad (\text{ec. 24})$$

Analogously:

$$\dot{Q}_{i \rightarrow j} = \frac{J_i - J_j}{R_{i \rightarrow j}} \quad [W]$$

Where:

$$R_{i \rightarrow j} = \frac{1}{A_i F_{i \rightarrow j}} = \text{Space resistance to radiation} \quad [21]$$

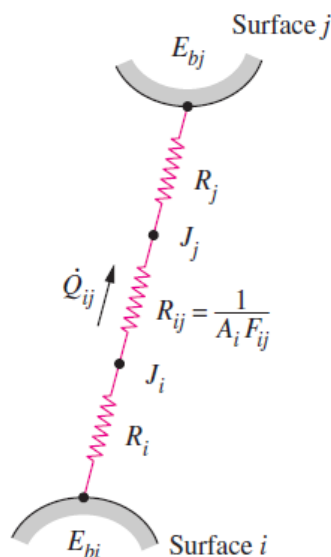


Figure 48: Space resistance to radiation [21]





## 5. Orbits

Varieties of orbits are used for different types of Earth-oriented missions. The most common orbits, in order of increasing altitude, are low Earth (LEO), Molniya, and geosynchronous (GEO).

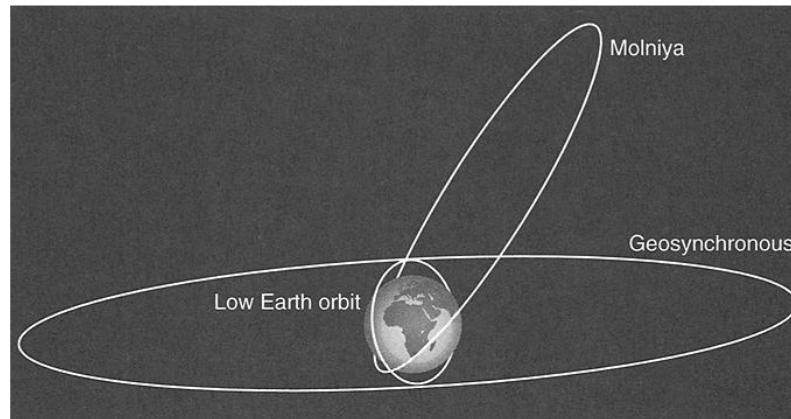


Figure 49: Classical earth orbits [22]

Orbits whose maximum altitudes are less than approximately 2000 km are considered low Earth orbits. They have the shortest periods, something like an hour and a half. Some of these orbits are circular, while others may be somewhat elliptical. The degree of eccentricity is limited by the fact that the orbit is not much larger than Earth, whose diameter is approximately 12,760 km. The inclination of these orbits, which is the angle between the plane of the equator and the plane of the orbit, can vary from  $0^\circ$  to greater than  $90^\circ$ . Inclinations greater than  $90^\circ$  cause a satellite in LEO to orbit in a direction opposite to Earth's rotation. Low Earth orbits are very often given high inclinations so that the satellite can pass over the entire surface of Earth from pole to pole as it orbits. This coverage is important for weather and surveillance missions.

The next higher type of common orbit is known as Molniya. These orbits are highly elliptical (apogee 38,900 km, perigee 550 km) and highly inclined ( $62^\circ$ ). They provide good views of the north polar region for a large portion of the orbit. Because the satellite travels very slowly near apogee, it has a good view of the polar region for up to eight hours out of its 12-hour period. A constellation of three satellites in Molniya orbits can provide continuous coverage of the northern hemisphere for missions such as communication with aircraft flying over the polar region.

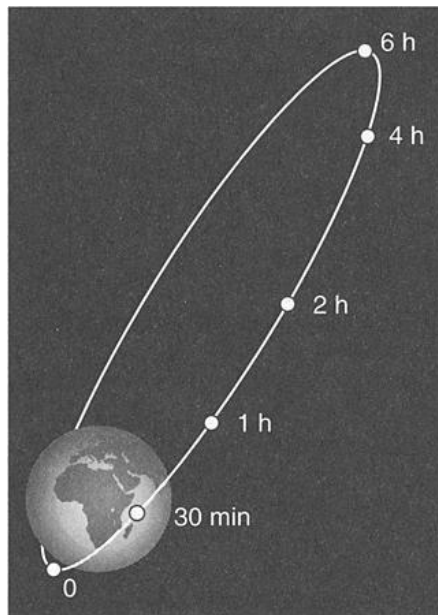


Figure 50: Molniya orbit [22]

The highest common orbit type is geosynchronous. These orbits are circular and have very low inclinations ( $< 10^\circ$ ). They have an altitude of 35,786 km. Their distinguishing characteristic is a period matching Earth's rotation, which allows a satellite to remain over the same spot on Earth at all times. This characteristic is valuable for a wide variety of missions, including weather observation, communication, and surveillance.

One final useful observation is that most Earth-orbiting satellites travel through their orbits in a counterclockwise motion as seen from above the North Pole. They move in this direction to take advantage of the initial eastward velocity given to the satellite as a result of Earth's rotation (approximately 1500 km/h at the Kennedy Space Centre). To travel the orbit in the opposite direction would require the booster to overcome the initial 1500 km/h eastward velocity before starting to build up speed in a westerly direction. This requirement would significantly affect booster size and allowable payload weight [22].

Besides that, the interplanetary orbits also exist and they are used in a wider range of missions that involve complicated trajectories. For this project, this analysis will not be of any interest.

Before going into a deeper analysis of the LEO orbit some terms must be described:

**Equatorial plane:** the plane of Earth's equator, which is perpendicular to Earth's spin axis.



**Ecliptic plane:** The plane of Earth's orbit around the sun. From the point of view of Earth, the sun always lies in the ecliptic plane. Over the course of a year, the sun appears to move continuously around Earth in this plane. Because of the tilt of Earth's spin axis, the equatorial plane is inclined  $23.4^\circ$  from the ecliptic plane, shown in Fig. 51 as the angle  $\delta$ .

**Sun day angle:** The position angle of the sun in the ecliptic plane measured from vernal equinox. At vernal equinox this angle is  $0^\circ$ , at summer solstice  $90^\circ$ , at autumnal equinox  $180^\circ$ , and at winter solstice  $270^\circ$ . This angle is shown as  $\psi$  in Fig. 51 and should not be confused with the "right ascension" of the sun, which is measured in the equatorial plane and is slightly different on most days of the year.

**Orbit inclination:** The angle between the orbit plane and the equatorial plane, shown as  $RI$  in Fig.51. Orbit inclinations typically vary from  $0^\circ$  to  $98^\circ$ , although inclinations greater than  $98^\circ$  are possible. For inclinations less than  $90^\circ$ , the satellite appears to be going around its orbit in the same direction as Earth's rotation. For inclinations greater than  $90^\circ$ , it appears to be going opposite Earth's rotation. In this case, its orbit is known as a retrograde orbit.

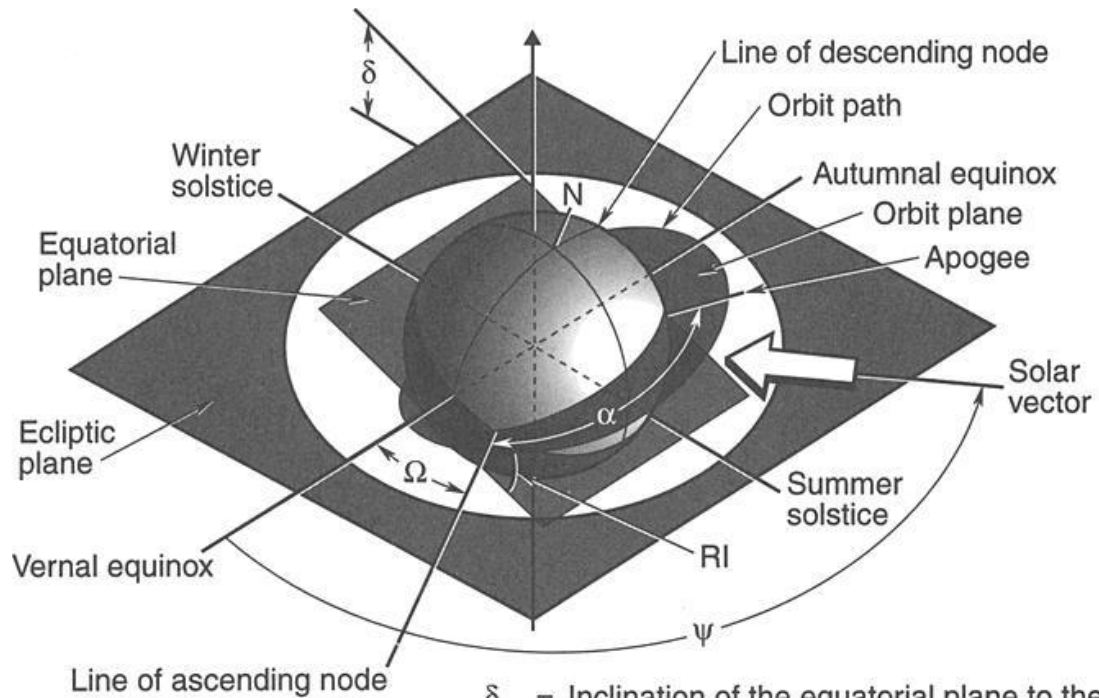
**Altitude:** the distance of a satellite above Earth's surface.

**Apogee/perigee:** Apogee is the point of highest altitude in an orbit and perigee, the lowest.

**Ascending node/descending node:** The ascending node is the point in the orbit at which the spacecraft crosses Earth's equator while traveling from south to north (i.e., when it is "ascending"). The descending node is the point crossed during the southbound portion of the orbit.

**Right ascension and declination:** The position of an object in the celestial coordinate system. Right ascension is the position angle in the equatorial plane measured from vernal equinox. Declination is the position angle above or below the equatorial plane.

**Right ascension of the ascending node (RAAN):** The position angle of the ascending node measured from vernal equinox in the equatorial plane ( $\Omega$  in Fig. 51). Earth's equatorial bulge causes the ascending and descending nodes to drift slightly on each revolution about Earth. (Earth is not a true sphere.) This drifting is known as "nodal regression." For most orbits, the RAAN drifts continuously with time and varies from  $0$  to  $360^\circ$ .



- $\delta$  = Inclination of the equatorial plane to the ecliptic plane
- $\Omega$  = Right ascension of the ascending node
- $\alpha$  = Argument of apogee
- $\psi$  = Sun day angle
- RI = Orbit inclination to the equatorial plane
- AA =  $(R_a + R_p)/2$
- EE =  $1 - R/AA$

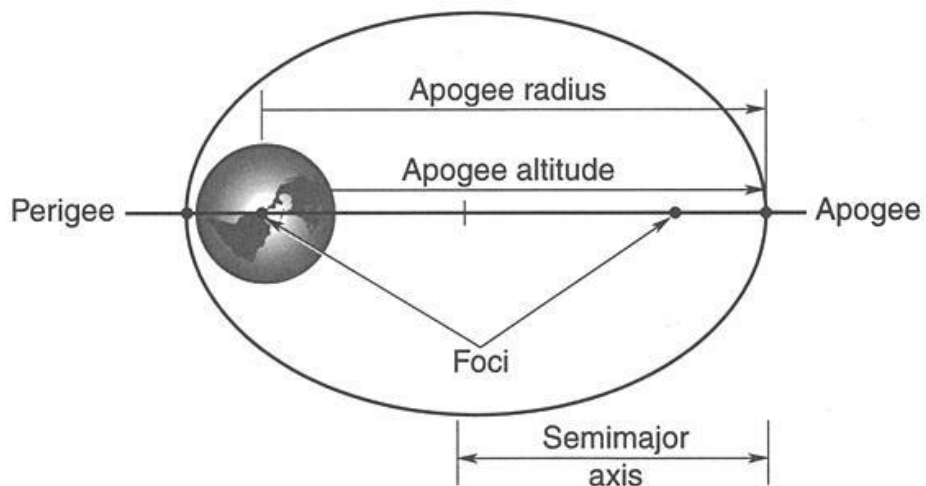


Figure 51: Orbital Parameters [22]



**Semimajor axis:** the semimajor axis of the orbit ellipse.

$$a = \frac{r_a + r_p}{2} \quad (ec. 25)$$

Where  $a$  is the orbit semimajor axis,  $r_a$  is the orbit radius at apogee (Earth's radius + apogee altitude), and  $r_p$  is the orbit radius at perigee (Earth's radius + perigee altitude).

**Period:** The time required to make one revolution about the Earth. As orbit altitude increases, so does the period. The orbit period may be calculated using the relation:

$$P = 2\pi \left( \frac{a^3}{\mu} \right)^{1/2} \quad (ec. 26)$$

Where  $P$  is the period,  $\mu$  is the product of the universal gravitational constant and the mass of the planet (for Earth,  $\mu = 3.98603 \times 10^{14} \text{ m}^3/\text{s}^2$ ), and  $a$  is the semimajor axis of the orbit (for a circular orbit, this is the orbit radius). The period of circular orbits versus orbit altitude is plotted in Fig. 52.

**Eccentricity:** The degree of oblateness of the orbit, defined as the ratio of one-half the interfocal distance to the semimajor axis. For a circular orbit, the eccentricity is 0. As the orbit becomes more elliptical, the eccentricity increases. Eccentricity is related to the apogee and perigee radii and the semimajor axis by the following relationships:

$$r_a = a(1 + e) \quad (ec. 27)$$

$$r_p = a(1 - e) \quad (ec. 28)$$

where  $r_a$  is the orbit radius at apogee,  $r_p$  is the orbit radius at perigee,  $a$  is the orbit semimajor axis, and  $e$  is the eccentricity.

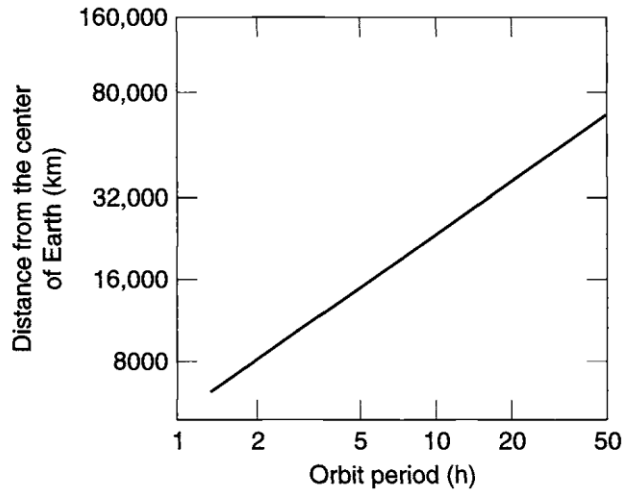


Figure 52: Total amount of time per orbit

**Argument of apogee:** For an elliptical orbit, the angle between the ascending node and apogee measured in the direction of satellite motion. This angle, shown as  $\alpha$  in Fig. 51, can vary from  $0^\circ$  to  $360^\circ$  [22].

### Orbit Beta Angle

Although the previous parameters are used by orbit and thermal analysts to describe particular orbits, another parameter, known as the orbit beta angle ( $\beta$ ), is more useful in visualizing the orbital thermal environment, particularly for low Earth orbits. The orbit beta angle is the minimum angle between the orbit plane and the solar vector, and it can vary from  $-90$  to  $+90$  deg, as illustrated in Fig. 53(a). The beta angle is defined mathematically as:

$$\beta = \sin^{-1}[\cos(\delta_s) \sin(RI) \sin(\Omega - \Omega_s)] + \sin(\delta_s) \cos(RI) \quad (ec. 29)$$

where  $\delta_s$  is the declination of the sun,  $RI$  is the orbit inclination,  $\Omega$  is the right ascension of the ascending node, and  $\Omega_s$  is the right ascension of the sun.

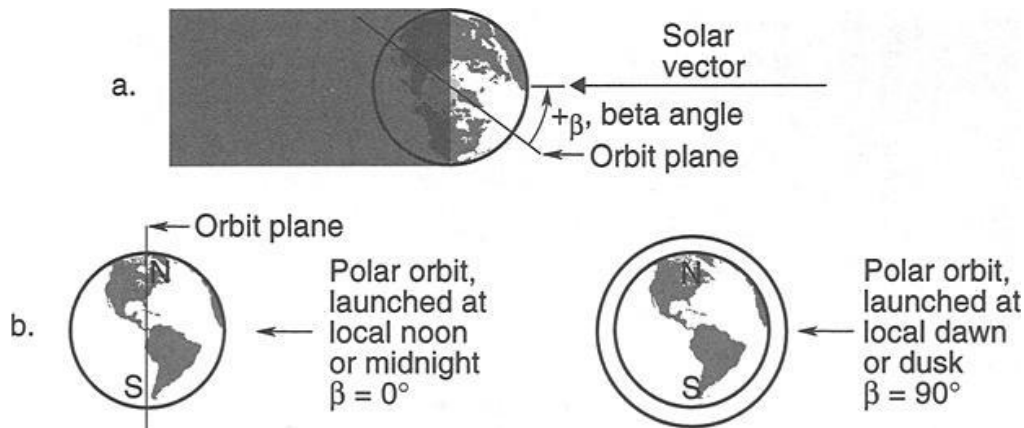


Figure 53: Orbit beta angle [22]

As viewed from the sun, an orbit with  $\beta$  equal to  $0^\circ$  appears edgewise, as shown in Fig. 53(b). A satellite in such an orbit passes over the subsolar point on Earth where albedo loads (sunlight reflected from Earth) are the highest, but it also has the longest eclipse time because of shadowing by the full diameter of Earth. As  $\beta$  increases, the satellite passes over areas of Earth further from the subsolar point, thereby reducing albedo loads; however, the satellite is also in the sun for a larger percentage of each orbit as a result of decreasing eclipse times. At some point, which varies depending on the altitude of the orbit, eclipse time drops to 0. With  $\beta$  equal to  $90^\circ$ , a circular orbit appears as a circle as seen from the sun; no eclipses exist, no matter what the altitude; and albedo loads are near 0. Fig.53 (b) shows how orbits of various beta angles appear as seen from the sun. Note that beta angles are often expressed as positive or negative; positive if the satellite appears to be going counterclockwise around the orbit as seen from the sun, negative if clockwise.

Figure 54 shows how eclipse times vary with  $\beta$  for circular orbits of different altitudes. The eclipse fraction of a circular orbit can be calculated from:

$$f_E = \frac{1}{180^\circ} \cos^{-1} \left[ \frac{(h^2 + 2Rh)^{\frac{1}{2}}}{(R + h)\cos\beta} \right] \quad \text{if } |\beta| < \beta^* \quad (\text{ec. 30})$$

$$f_E = 0 \quad \text{if } |\beta| \geq \beta^*$$

$$\beta^* = \sin^{-1} \left[ \frac{R}{R + h} \right] \quad 0^\circ \leq \beta^* \leq 90^\circ \quad (\text{ec. 31})$$



Where  $R$  is Earth's radius (6378 km),  $h$  is orbit altitude,  $\beta$  is orbit beta angle, and  $\beta^*$  is the beta angle at which eclipses begin.

Both equations assume Earth's shadow is cylindrical, which is valid for low orbits where no appreciable difference exists between the umbral and penumbral regions of total and partial eclipsing, respectively. For 12-hour and geosynchronous orbits, these equations may be slightly in error. For any given satellite,  $\beta$  will vary continuously with time because of the orbit nodal regression and the change in the sun's right ascension and declination over the year.

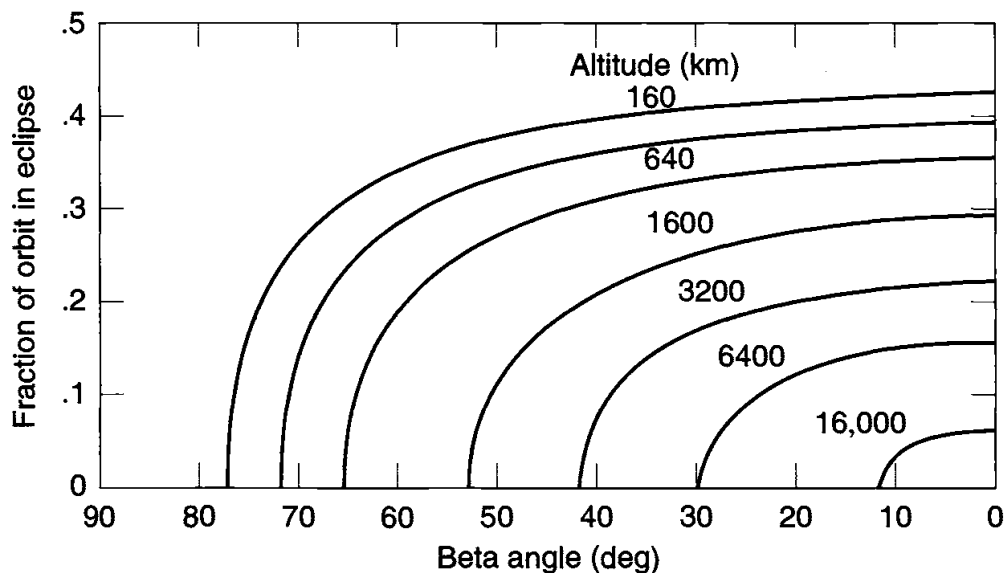


Figure 54: Eclipse durations [22]

More concretely, for low earth orbits, the chief advantage in thinking in terms of  $\beta$  is that it simplifies the analysis of orbital thermal environments. By analyzing the environments at several discrete values, one can be confident that all possible combinations of orbit RAAN and sun day angles have been covered. Figure 55 shows such an analysis for a spinning cylindrical satellite in a 555-km-altitude LEO. Earth-emitted IR was considered constant over Earth and therefore independent of orbit inclination, RAAN, or  $\beta$ . The IR load to the satellite therefore is constant with  $\beta$ . Since the eclipse time decreases with  $\beta$ , however, the satellite spends more time in the sun, thereby increasing the orbit-average solar load, as shown in Fig. 55. In addition, as  $\beta$  increases, the albedo loads decrease, as can be seen by comparing the "solar" and "solar plus albedo" curves in Fig. 55. The net result for this particular satellite was that solar-panel orbit-





average temperature (which provides a radiative heat sink for the internal components) was a minimum at  $\beta = 0^\circ$  and a maximum at  $\beta = 65^\circ$  [22].

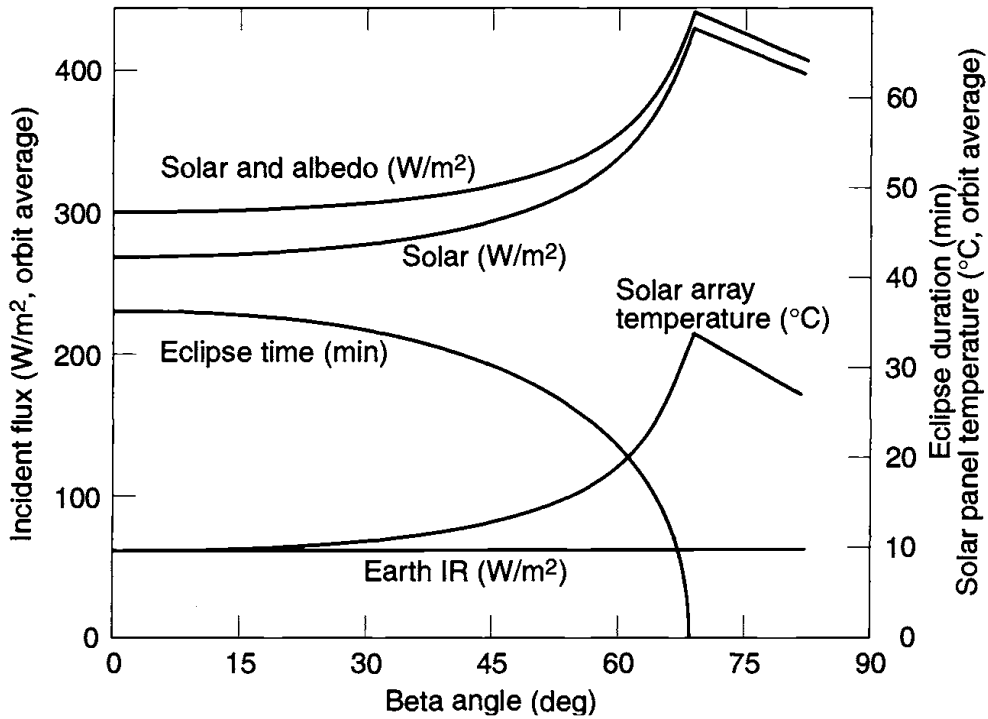


Figure 55: Cylinder in LEO [22]

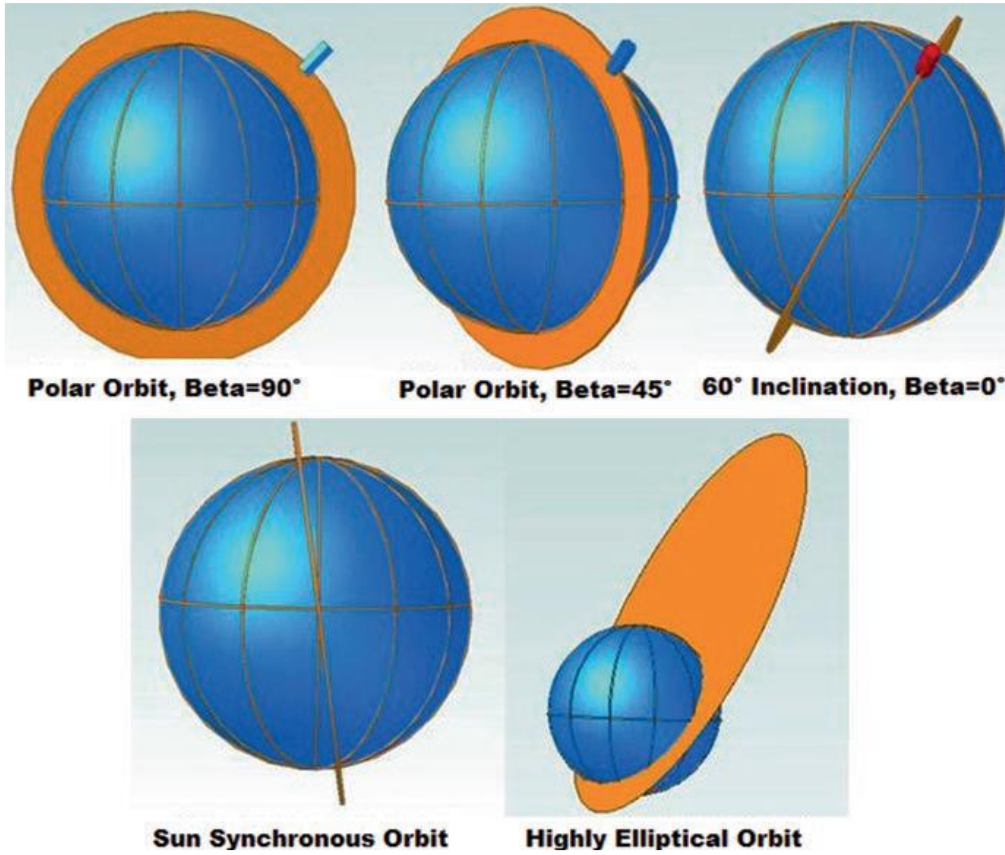


Figure 56: Seeing from the Sun beta changes [12]



## 6. Environments of Earth orbits

Spacecraft thermal control is a process of energy management in which environmental heating plays a major role. The principal forms of environmental heating on orbit are direct sunlight, sunlight reflected off Earth (albedo), and infrared (IR) energy emitted from Earth. During launch or in exceptionally low orbits, there is also a free molecular heating (FMH) effect caused by friction in the rarefied upper atmosphere.

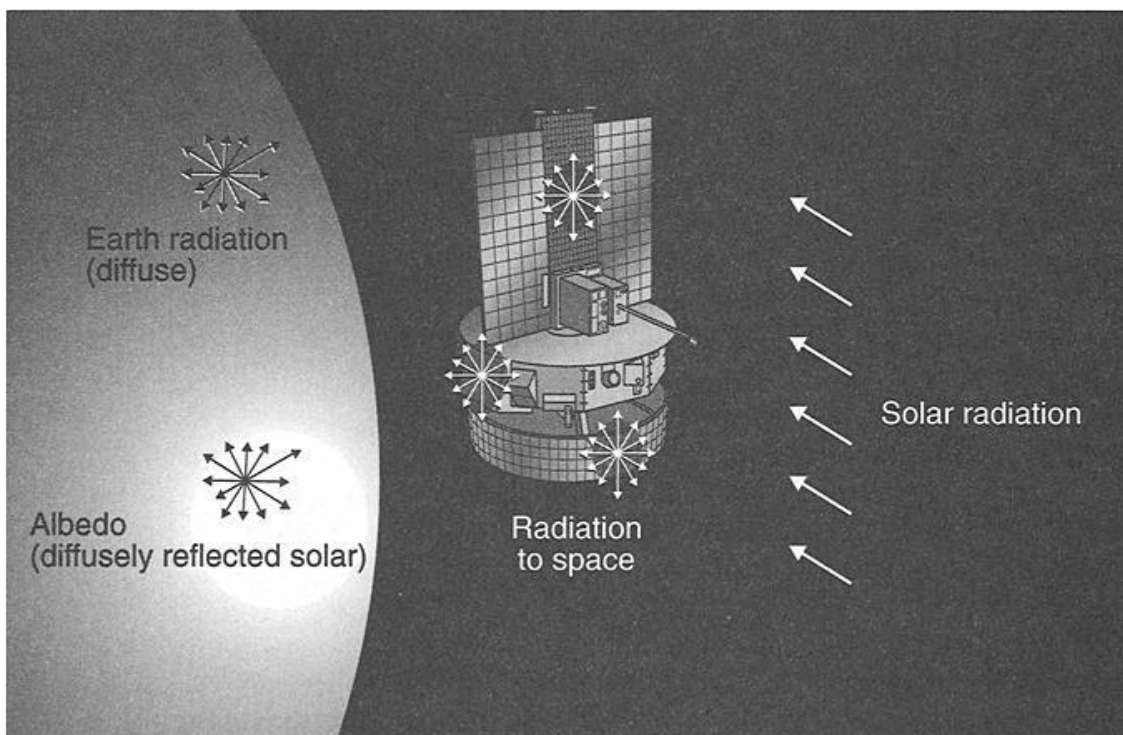


Figure 57: Heat sources [22]

In low Earth orbit (LEO), a space vehicle's altitude is small compared to the diameter of Earth. This means that a satellite views only a small portion of the full globe at any given time. The satellite's motion as it orbits therefore exposes it to rapidly changing environmental conditions as it passes over regions having different combinations of land, ocean, snow, and cloud cover. These short-duration swings in environmental conditions are not of much concern to massive, well-insulated spacecraft components. Exposed lightweight components such as solar arrays and deployable radiators, however, will respond to the extreme environments encountered for short time periods, so one must consider those environments in the design process. As the



following discussion shows, the shorter the thermal time constant a particular component has, the wider the range of environments that must be considered. [22]

### 6.1. Direct solar

Sunlight is the greatest source of environmental heating incident on most spacecraft in Earth orbit. Fortunately, the sun is a very stable energy source. Even the 11-year solar cycle has very little effect on the radiation emitted from the sun, which remains constant within a fraction of 1% at all times. However, because Earth's orbit is elliptical, the intensity of sunlight reaching Earth varies approximately +/- 3.5%, depending on Earth's distance from the sun. At summer solstice, Earth is farthest from the sun, and the intensity is at its minimum value of  $1322 \text{ W/m}^2$ ; at winter solstice, the intensity is at its maximum of  $1414 \text{ W/m}^2$ . The intensity of sunlight at Earth's mean distance from the sun (1 AU) is known as the solar constant and is equal to  $1367 \text{ W/m}^2$ . The above values are recommended by the World Radiation Center in Davos, Switzerland, and are believed accurate to within 0.4%.

Solar intensity also varies as a function of wavelength, as shown in Fig. 58. The energy distribution is approximately 7% ultraviolet, 46% visible, and 47% near (short-wavelength) IR, with the total integrated energy equal to the  $1322$  to  $1414 \text{ W/m}^2$  values mentioned above. An important point, however, is that the IR energy emitted by the sun is of a much shorter wavelength than that emitted by a body near room temperature. This distinction allows for the selection of thermal-control finishes that are very reflective in the solar spectrum but whose emissivity is high in the room-temperature (long-wavelength) IR portion of the spectrum. [22]

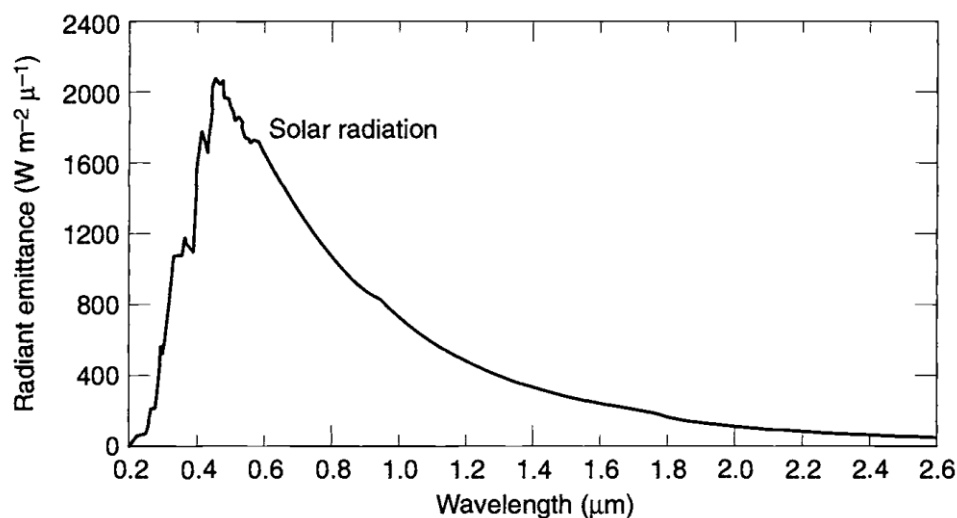


Figure 58: Emittance vs Wavelength [22]

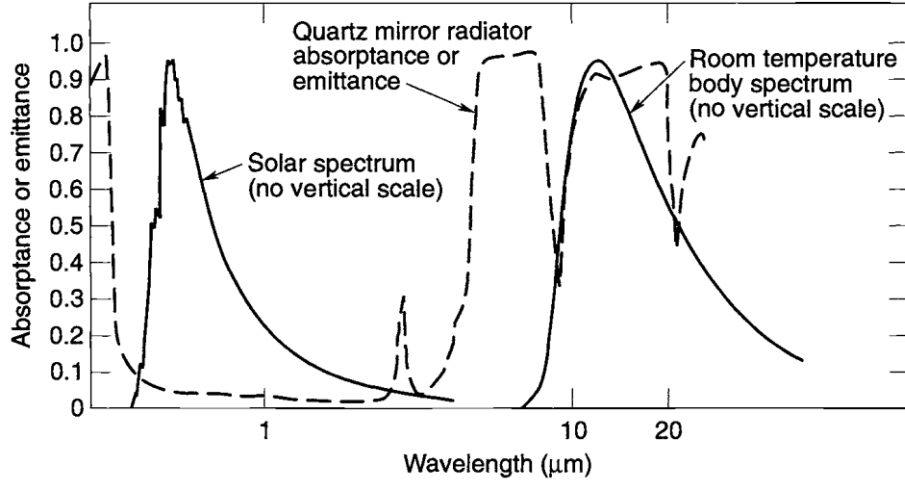


Figure 59: Absorbance vs Wavelength [22]

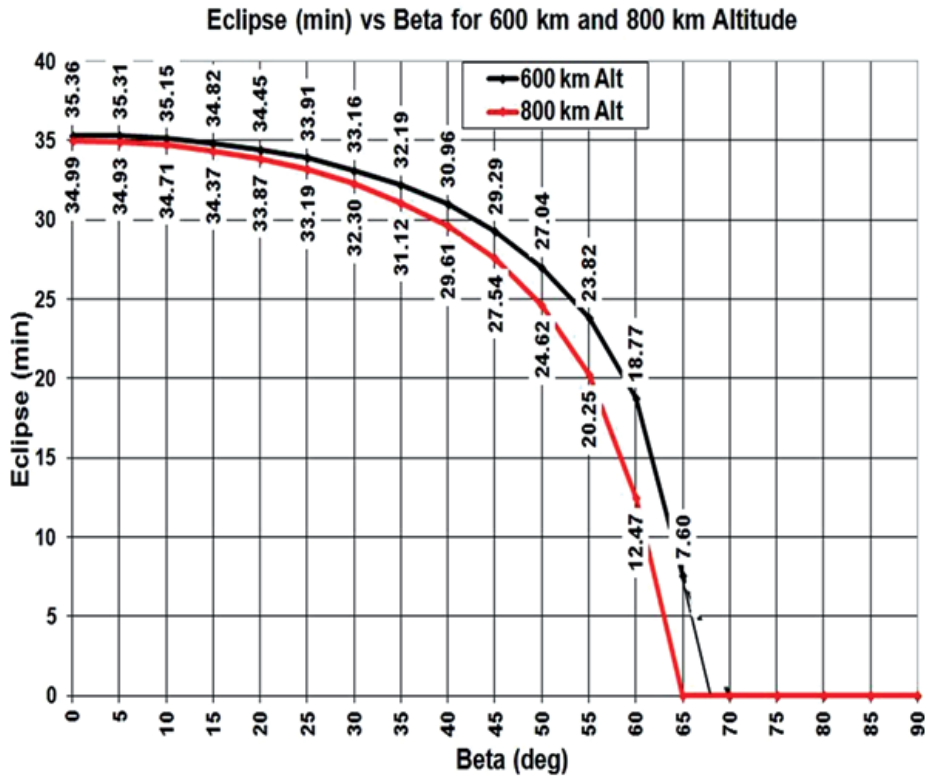


Figure 60: Eclipse time vs Beta degree[12]



## 6.2. Albedo

Sunlight reflected off a planet or moon is known as albedo. A planet's albedo is usually expressed as the fraction of incident sunlight reflected back to space, and it is highly variable. Usually, reflectivity is greater over continental regions than oceanic regions and generally increases with decreasing local solar-elevation angles and increasing cloud coverage. Because of greater snow and ice coverage, decreasing solar-elevation angle, and increasing cloud coverage, albedo also tends to increase with latitude. These variations make selection of the best albedo value for a particular thermal analysis rather uncertain, and variations throughout the industry are not unusual.

Another important point is that the albedo heat flux reaching a spacecraft will decrease as the spacecraft moves along its orbit and away from the subsolar point (the point on Earth or another planet where the sun is at the zenith, i.e., directly overhead), even if the albedo constant remains the same. This happens because the albedo factor is a reflectivity, not a flux. As the spacecraft moves away from the subsolar point it is over regions of Earth's surface where the local incident solar energy per square meter is decreasing with the cosine of the angle from the subsolar point. The albedo heat load on the spacecraft will therefore approach 0 near the terminator (the dividing line between the sunlit and dark sides of a planet), even if the albedo value (reflectivity) is 1.0. This geometric effect is accounted for by the analysis codes used to perform spacecraft thermal analysis. The analyst is just responsible for selecting the albedo (reflectivity) value itself. [22]

## 6.3. Earth IR

All incident sunlight not reflected as albedo is absorbed by Earth and eventually reemitted as IR energy. While this balance maintains itself fairly well on a global annual average basis, the intensity of IR energy emitted at any given time from a particular point on Earth can vary considerably depending on factors such as the local temperature of Earth's surface and the amount of cloud cover. A warmer surface region will emit more radiation than a colder area. Generally, highest values of Earth-emitted IR will occur in tropical and desert regions (as these are the regions of the globe receiving the maximum solar heating) and will decrease with latitude. Increasing cloud cover tends to lower Earth-emitted IR, because cloud tops are cold and clouds effectively block upwelling radiation from Earth's warmer surface below. These



localized variations in Earth-emitted IR, while significant, are much less severe than the variations in albedo.

The IR energy emitted by Earth, which has an effective average temperature around  $-18^{\circ}\text{C}$ , is of approximately the same wavelength as that emitted by a spacecraft; that is much larger wavelength than the energy emitted by the sun at  $5500^{\circ}\text{C}$ . Unlike short-wavelength solar energy, Earth IR loads incident on a spacecraft cannot be reflected away from radiator surfaces with special thermal-control coatings, since the same coatings would prevent the radiation of waste heat away from the spacecraft. Because of this, Earth-emitted IR energy can present a particularly heavy backload on spacecraft radiators in low-altitude orbits.

The concept of Earth-emitted IR can be confusing, since the spacecraft is usually warmer than the effective Earth temperature, and the net heat transfer is from spacecraft to Earth. However, for analysis, a convenient practice is to ignore Earth when calculating view factors from the spacecraft to space and to assume that Earth does not block the view to space. Then the difference in IR energy is added back in as an "incoming" heat rate called Earth-emitted IR. [22]

Leo thermal environment:

	<b>Perihelion</b>	<b>Aphelion</b>	<b>Mean (Hot Case)</b>	<b>Eclipse (Cold Case)</b>
Direct Solar	1414 $\text{W}/\text{m}^2$	1323 $\text{W}/\text{m}^2$	1371 $\text{W}/\text{m}^2$	0
Albedo (average)	0.30 $\pm$ 0.01	0.30 $\pm$ 0.01	0.30 $\pm$ 0.01	0.25
Planetary IR (average)	234 $\pm$ 7 $\text{W}/\text{m}^2$	234 $\pm$ 7 $\text{W}/\text{m}^2$	234 $\pm$ 7 $\text{W}/\text{m}^2$	220 $\text{W}/\text{m}^2$

Table 18: LEO thermal Environment [23]

Where: hot case is during direct sunlight and cold case during eclipse

#### 6.4. Molecular free heating

Another significant form of environmental heating is free molecular heating (FMH). This kind of heating is a result of bombardment of the vehicle by individual molecules in the outer reaches of the atmosphere. For most spacecraft, FMH is only encountered during launch ascent just after





the booster's payload fairing is ejected. A desirable practice is to drop the fairing as soon as possible after launch to minimize the amount of dead weight the booster must deliver to orbit. The point at which the fairing is separated is often determined by a trade-off between the desire to save weight and the need to protect the payload spacecraft from excessive atmospheric heating.

Fairing separation always occurs at altitudes high enough for the resultant heating to be in the free or near-free molecular regime; that is, the heating is modelled as collisions of the body with individual molecules rather than as a gas-flow heating problem. The heating rate is given by:

$$Q_{FMH} = \alpha \left( \frac{1}{2} \right) \rho V^3 \quad (ec. 32)$$

where  $\rho$  is atmospheric density,  $V$  is vehicle velocity, and  $\alpha$  is the accommodation coefficient (approximately 0.6 to 0.8, but a value of 1.0 is recommended for conservatism).

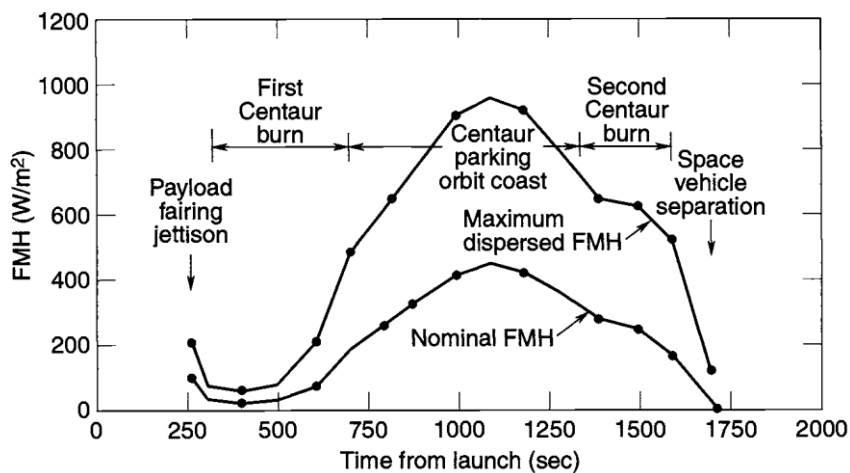


Figure 61: FMH

Although this source of heat is very important for the launch part, it is not during operation of the spacecraft, so for this analysis it will not be considered.

### 6.5. Charged-particle heating

Charged particles constitute an additional heating source, although weak compared to the four principal environmental heating sources discussed above and generally not significant in the thermal design of room-temperature systems. At cryogenic temperatures, however, charged-particle heating can become a significant factor in thermal design because of the high sensitivity of such systems to environmental heat loads.





The near-Earth trapped charged particles, known as the Van Allen belts, lie about the plane of the geomagnetic equator and feature relativistic electrons and protons. The spatial characteristics of the Van Allen belts and the spectral properties of the trapped particles within them undergo both regular and irregular variations with time, accounted for by the solar-activity level. The bulk of the Van Allen belts is approximately bounded by altitudes of 6500 and 52,000 km. This fact makes this source negligible for this analysis.



*Page intentionally left in blank*